UNDERSTANDING NEUTRON STARS WITH GRAVITATIONAL WAVES

NIKOLAOS STERGIOULAS

main collaborators: A. BAUSWEIN, J. CLARK, T. JANKA

DEPARTMENT OF PHYSICS
ARISTOTLE UNIVERSITY OF THESSALONIKI

Rethymno, July 1, 2015

Neutron Stars

First neutron star detected almost 50 years ago. Still, the fundamental properties of matter in the core of neutron stars remain largely uncertain.

No accurate radius determination!

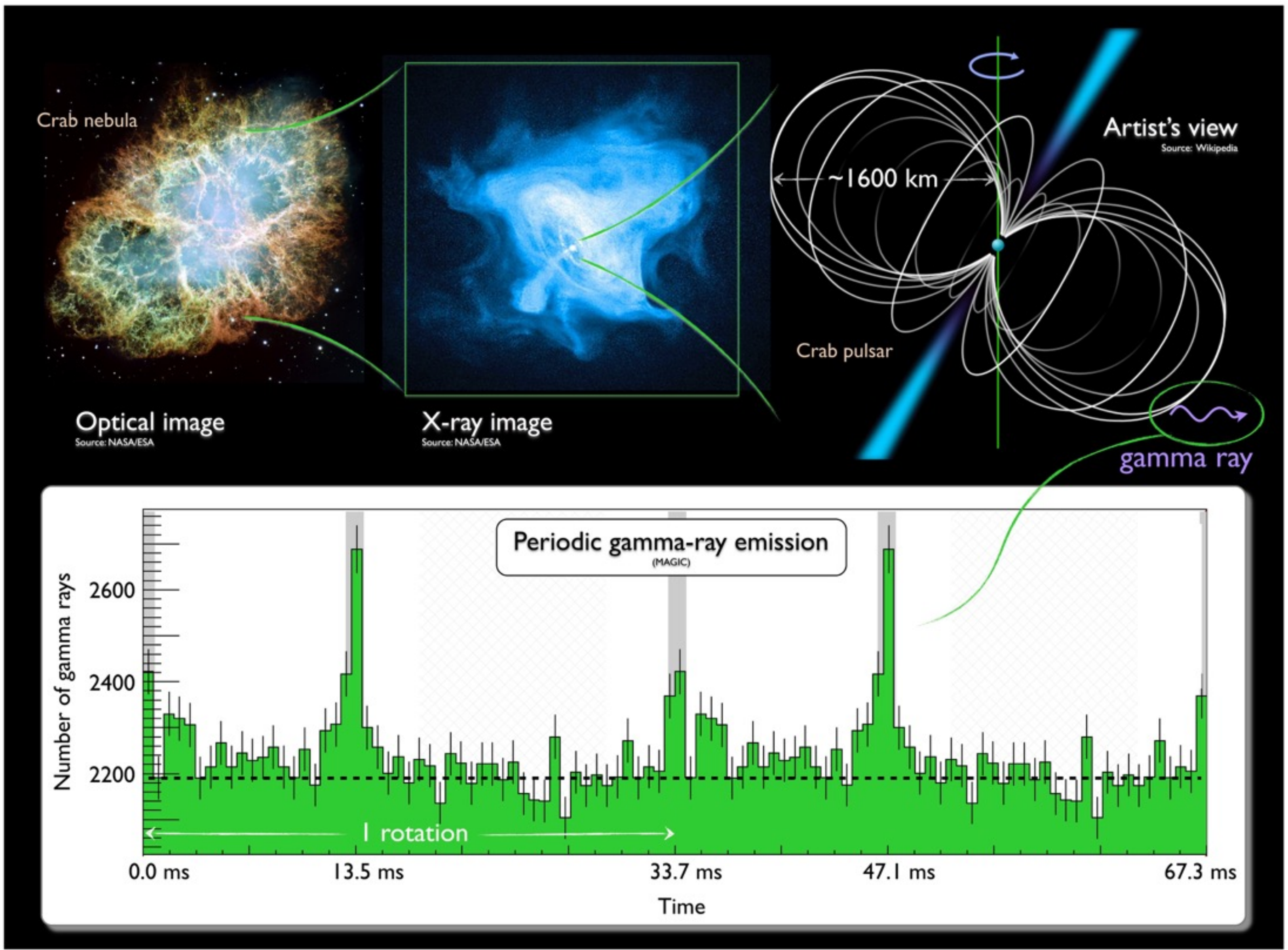

Image credit: MAGIC collaboration

Sample of Neutron Star Equations of State

Bauswein, Janka, Hebeler & Schwenk (2012)

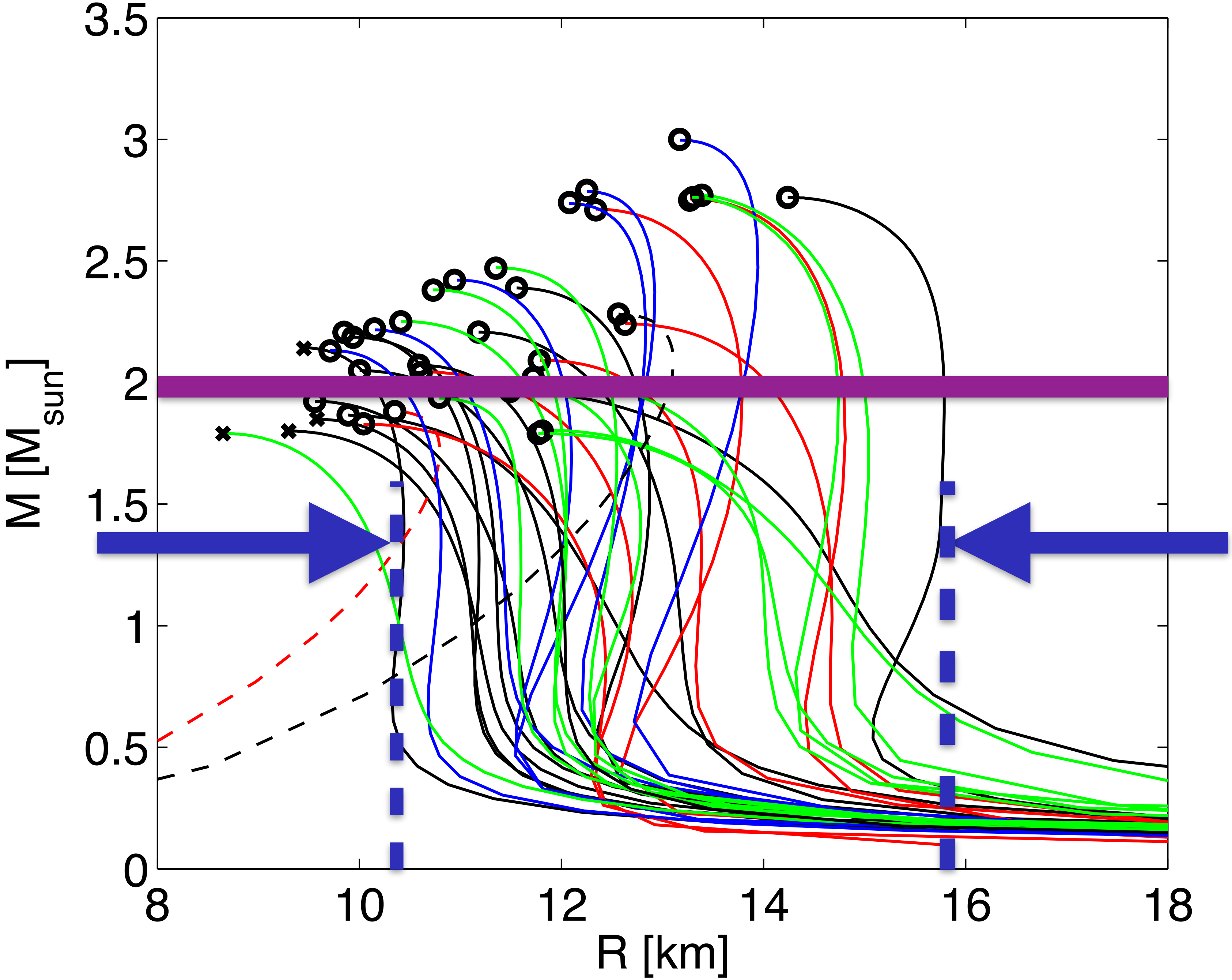

Constraints on Neutron Star Radii

Main methods in EM spectrum:

- Thermonuclear X-ray bursts (photospheric radius expansion)
- Burst oscillations (rotationally modulated waveform)
- Fits of thermal spectra to cooling neutron stars
- khZ QPOs in accretion disks around neutron stars
- Pericenter precession in relativistic binaries (double pulsar J0737)

Main methods in GW spectrum:

- Tidal effects on waveform during inspiral phase of NS-NS mergers
- Tidal disruption in BH-NS mergers
- Oscillations in post-merger phase of NS-NS mergers

EOS from Inspiral Signal

Read et al. (2013)

The last part of the inspiral signal carries the imprint of the quadrupole *tidal deformability* $\lambda := -Q_{ij}/E_{ij} = 2/3\, k_2\, R^5$.

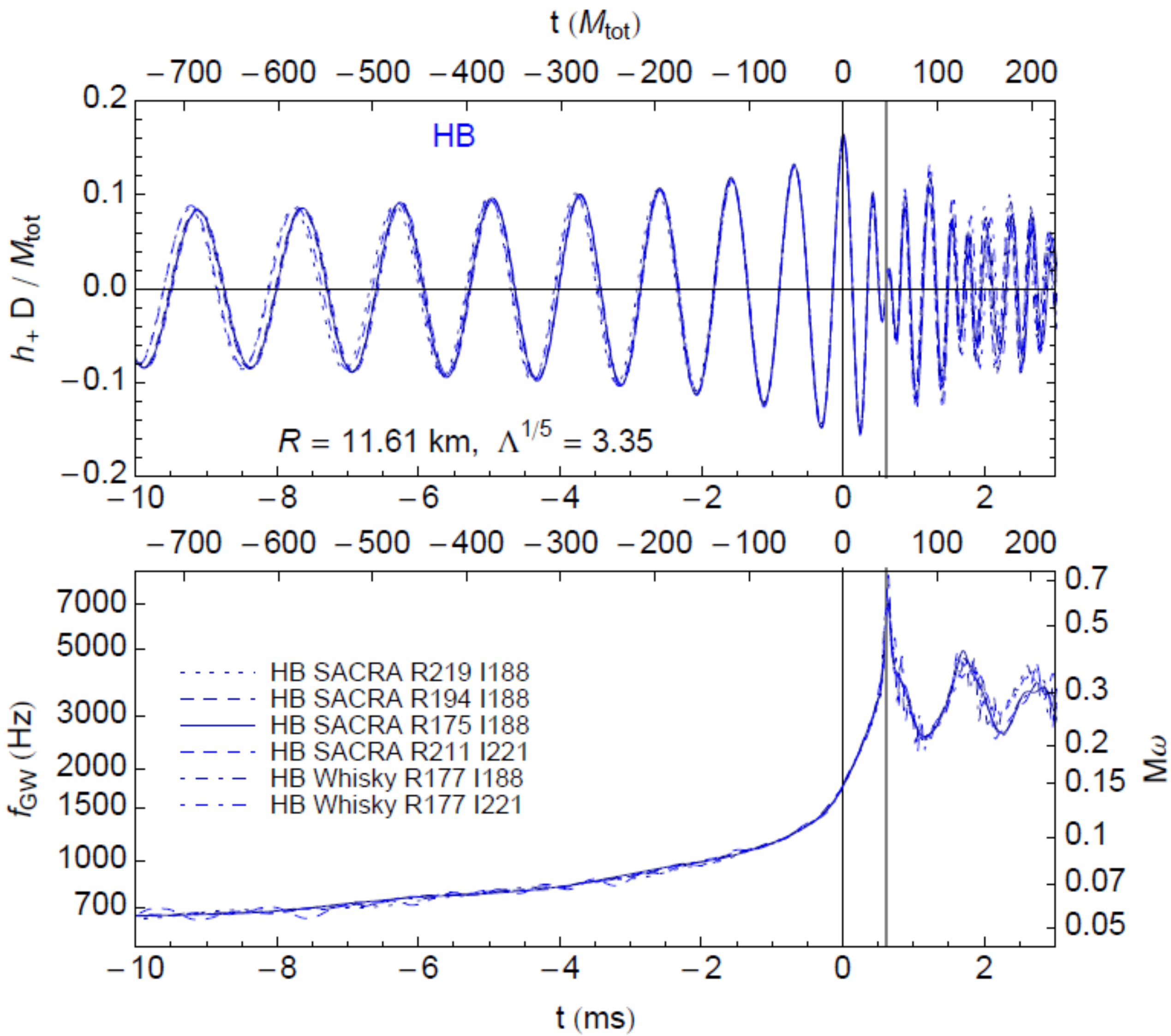

k_2 = tidal Love number

Dimensionless tidal deformability:

$$\Lambda \equiv \frac{2}{3} k_2 \left(\frac{R}{M}\right)^5$$

With an aLIGO class detector:

ΔR/R ~ 10 %

@100 Mpc

Revealing the EOS

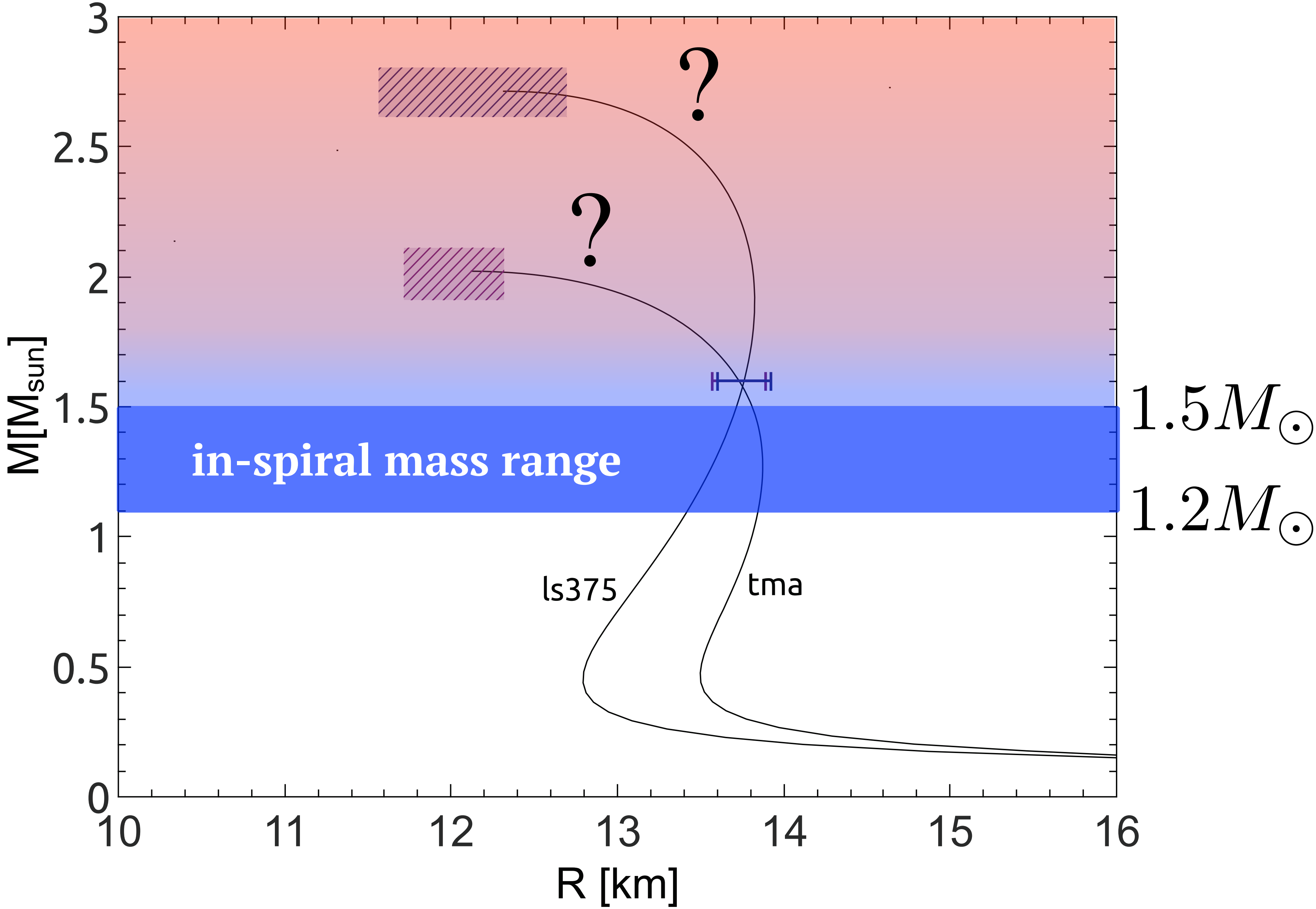

Outcome of Binary NS Mergers

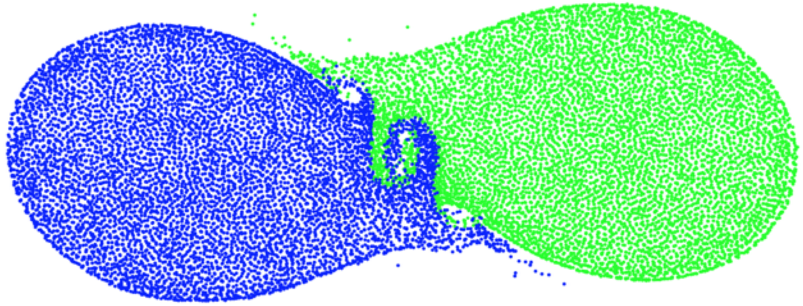

Most likely range of total mass for binary system:

$$2.4 M_\odot < M_{\rm tot} < 3 M_\odot$$

Because nonrotating $M_{\rm max} > 2M_\odot$ (as required by observations), a long-lived (τ >10ms) remnant is likely to be formed.

The remnant is a *hypermassive neutron star (HMNS)*, supported by *differential rotation*, with a mass larger than the maximum mass allowed for uniform rotation.

Simulations of BNS mergers

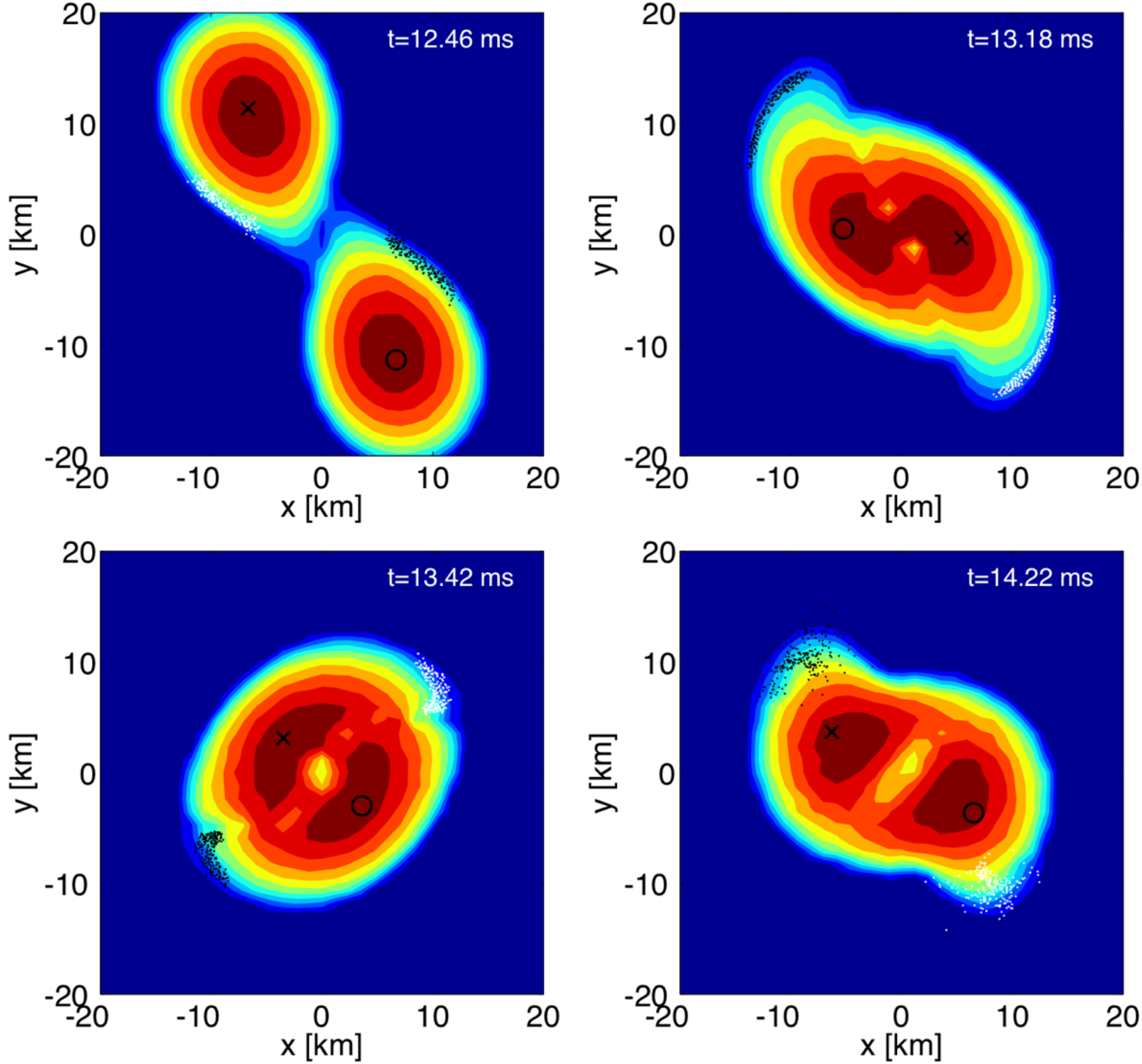

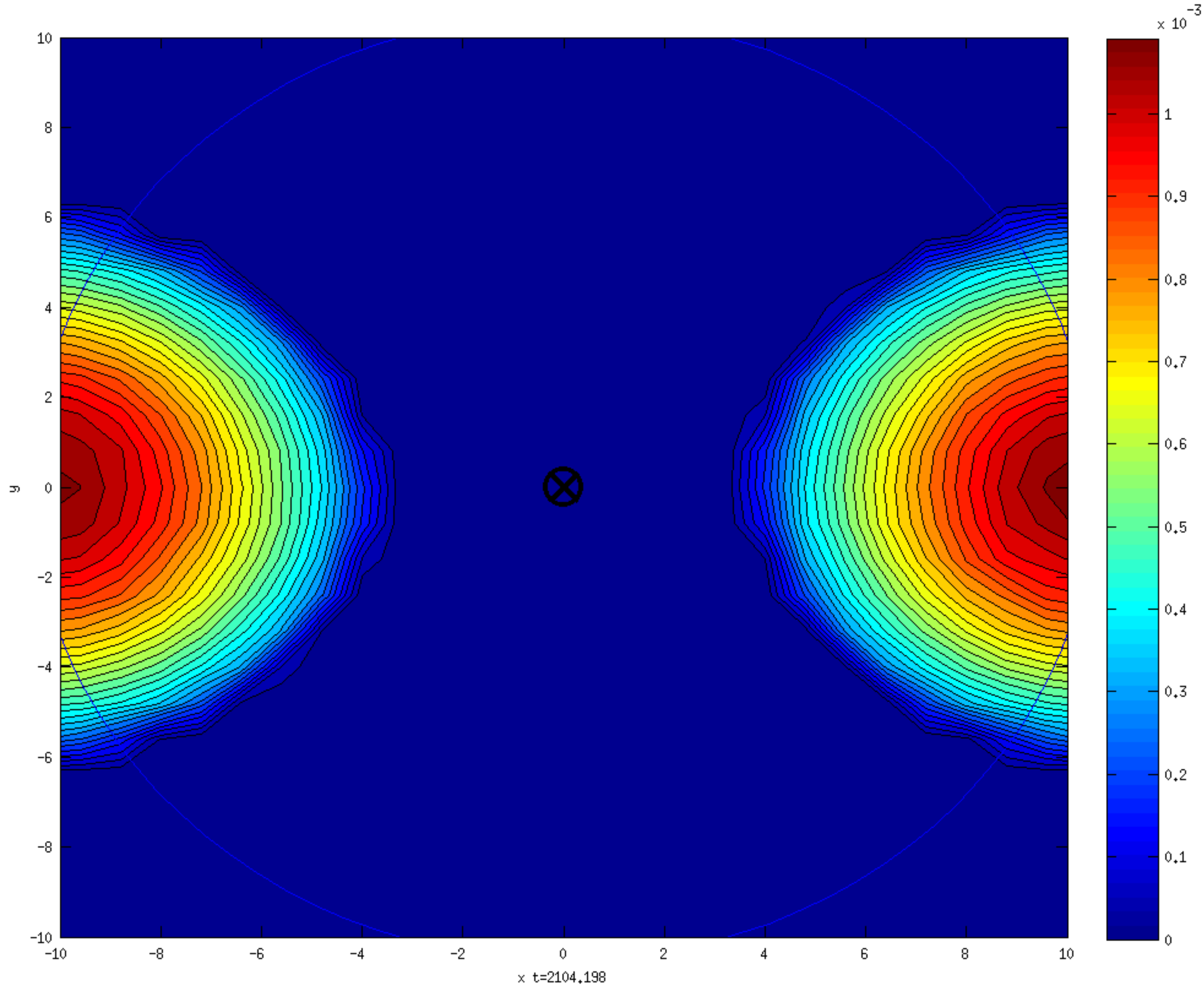

x 10^-3
1
0.9
0.8
0.7
0.6
0.5
0.4
0.3
0.2
0.1
0
10
8
6
4
2
0
-2
-4
-6
-8
-10
y
-10
-8
-6
-4
-2
0
2
4
6
8
10
x t=2104.198

Post-Merger Gravitational Waves

The GW signal can be divided into three distinct phases:
inspiral, *merger* and *post-merger ringdown*. *(@40Mpc)*

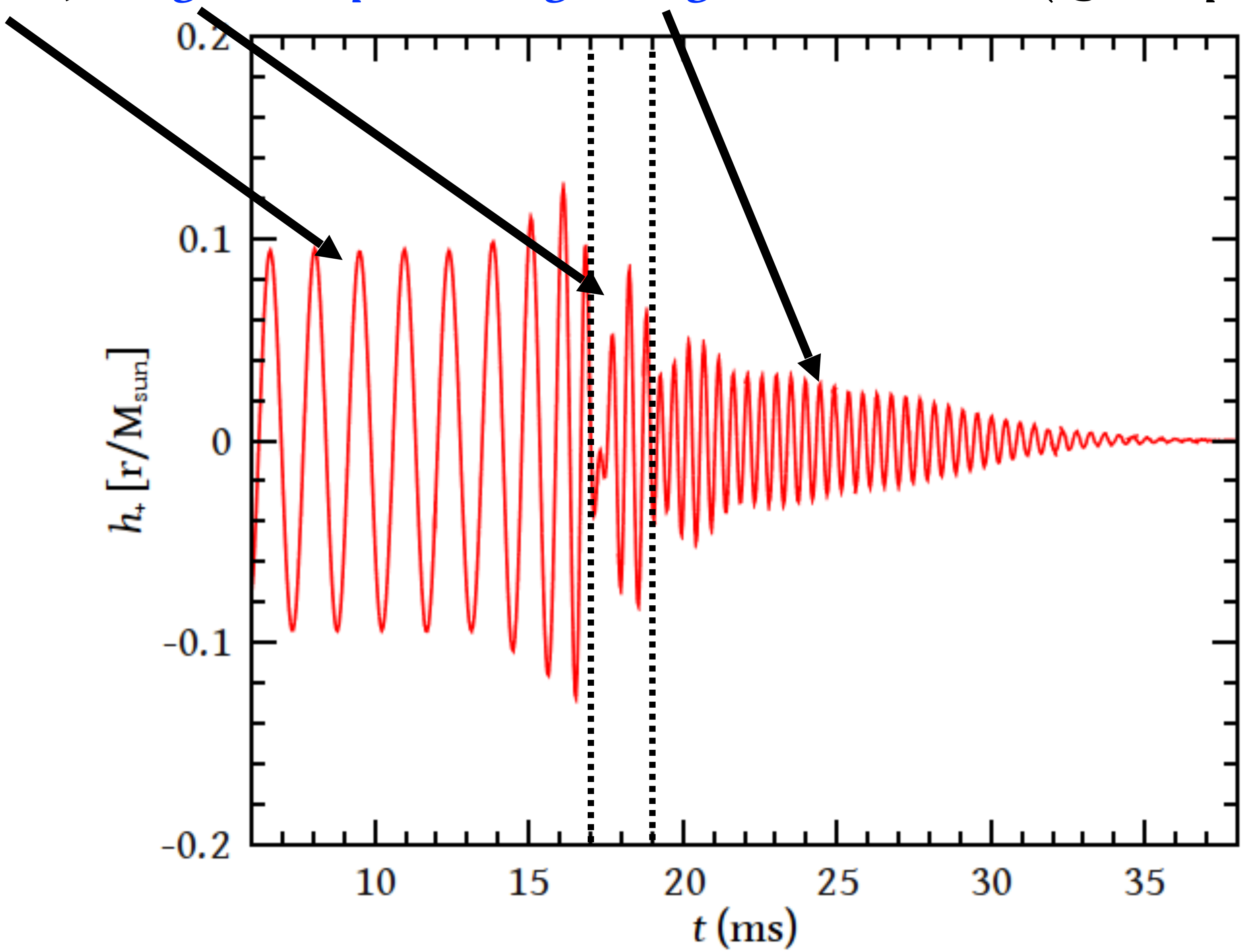

Post-Merger GW Spectrum

Several peaks stand above the aLIGO/VIRGO or ET sensitivity curves and are potentially detectable. How are these produced?

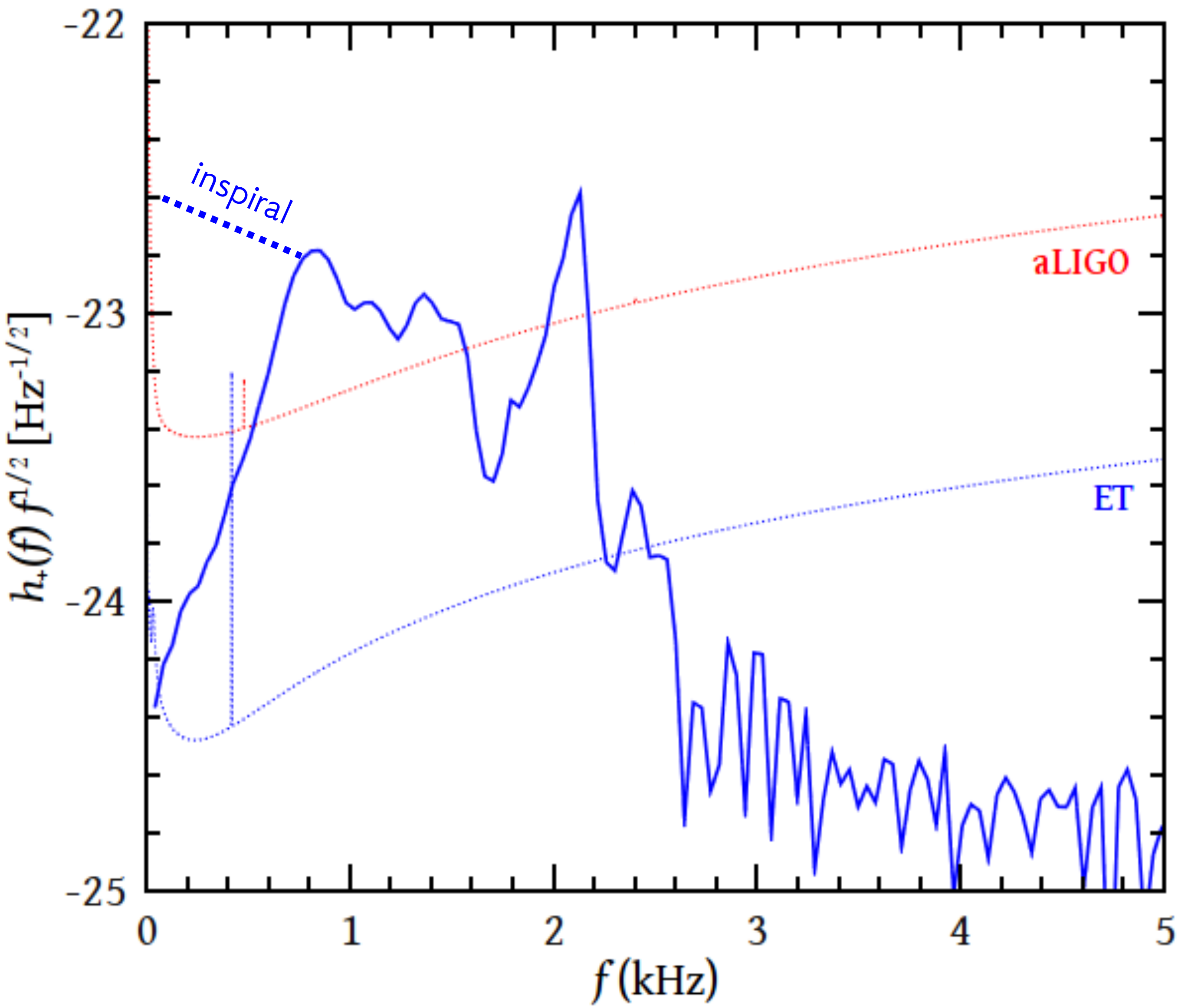

Oscillations of Neutron Stars

$$\boldsymbol{\xi}(r,\theta,\phi) = \sum_{l=0}^{\infty}\sum_{m=-l}^{l}\left[U_l^m(r)Y_l^m(\theta,\phi)\hat{\mathbf{e}}_r + V_l^m(r)\nabla Y_l^m(\theta,\phi) + W_l^m(r)\hat{\mathbf{e}}_r \times \nabla Y_l^m(\theta,\phi)\right]$$

Main oscillation modes:

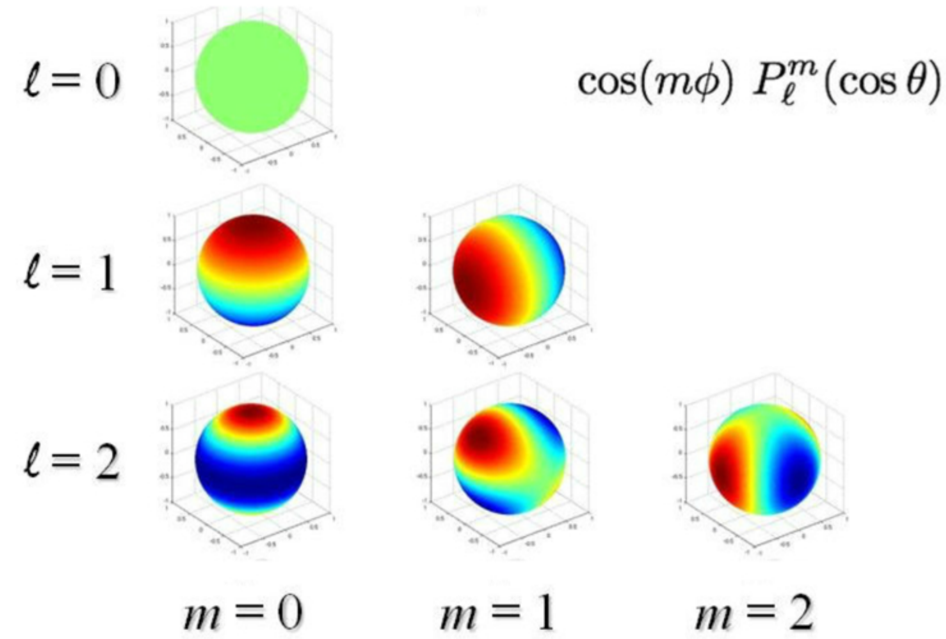

1. *f*-modes / *p*-modes

   fluid modes restored by pressure

2. *g*-modes

   restored by gravity/buoyancy

3. inertial modes (*r*-modes)

   restored by the Coriolis force in *rotating* stars

4. *w*-modes

   spacetime modes (similar to black hole modes)

GW-detection: *f*-modes: stable oscillations

f-mode / *r*-mode *CFS*-instabilities

The *l*=*m*=2 linear *f*-mode

Re-excitation of (co-rotating) *l*=*m*=2 linear *f*-mode in the post-merger remnant at ~20ms after merger.

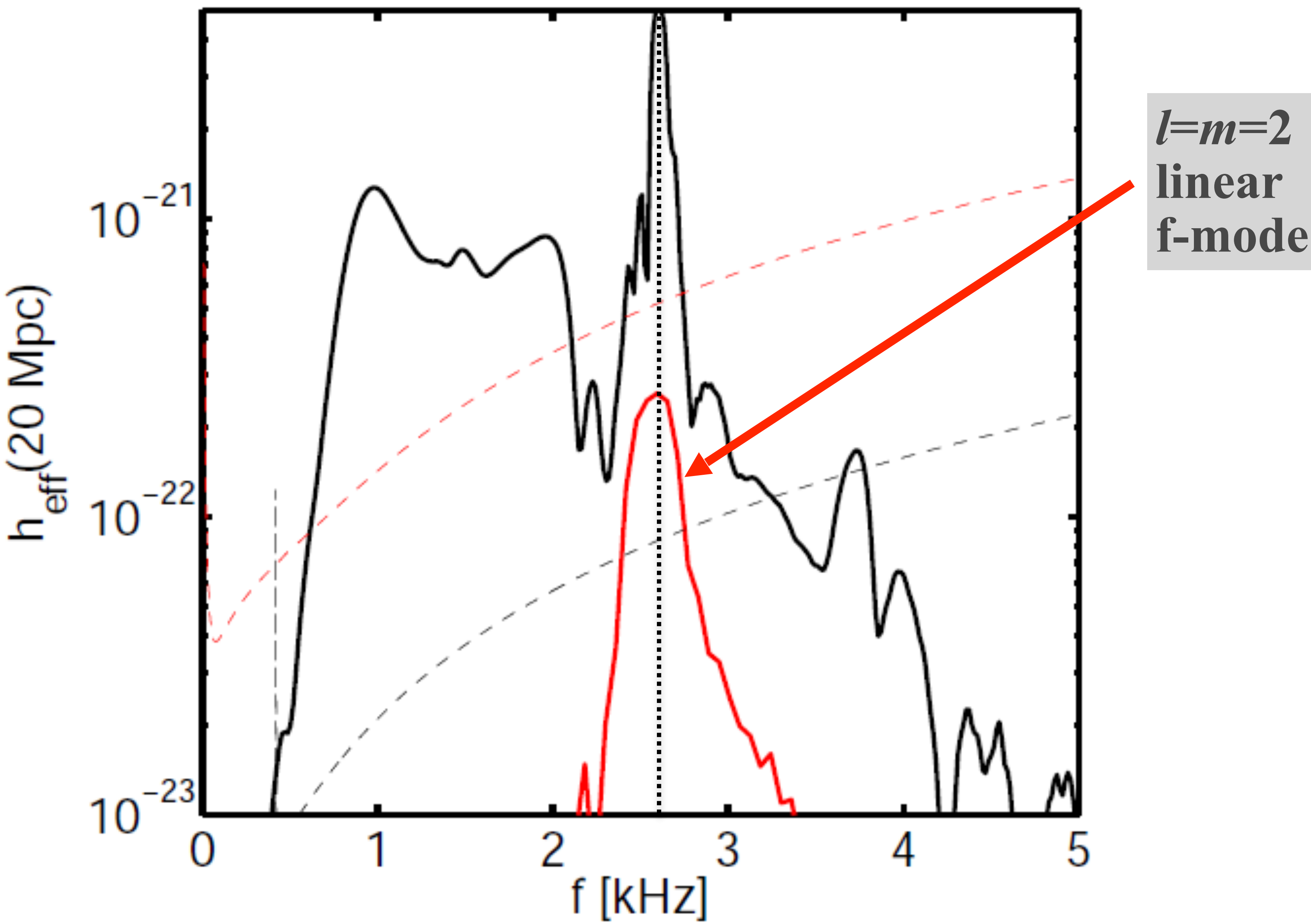

The *l*=*m*=2 linear *f*-mode

Structure of the *l*=*m*=2 linear *f*-mode in the equatorial plane.

NS, Bauswein, Zagkouris, Janka (2011)

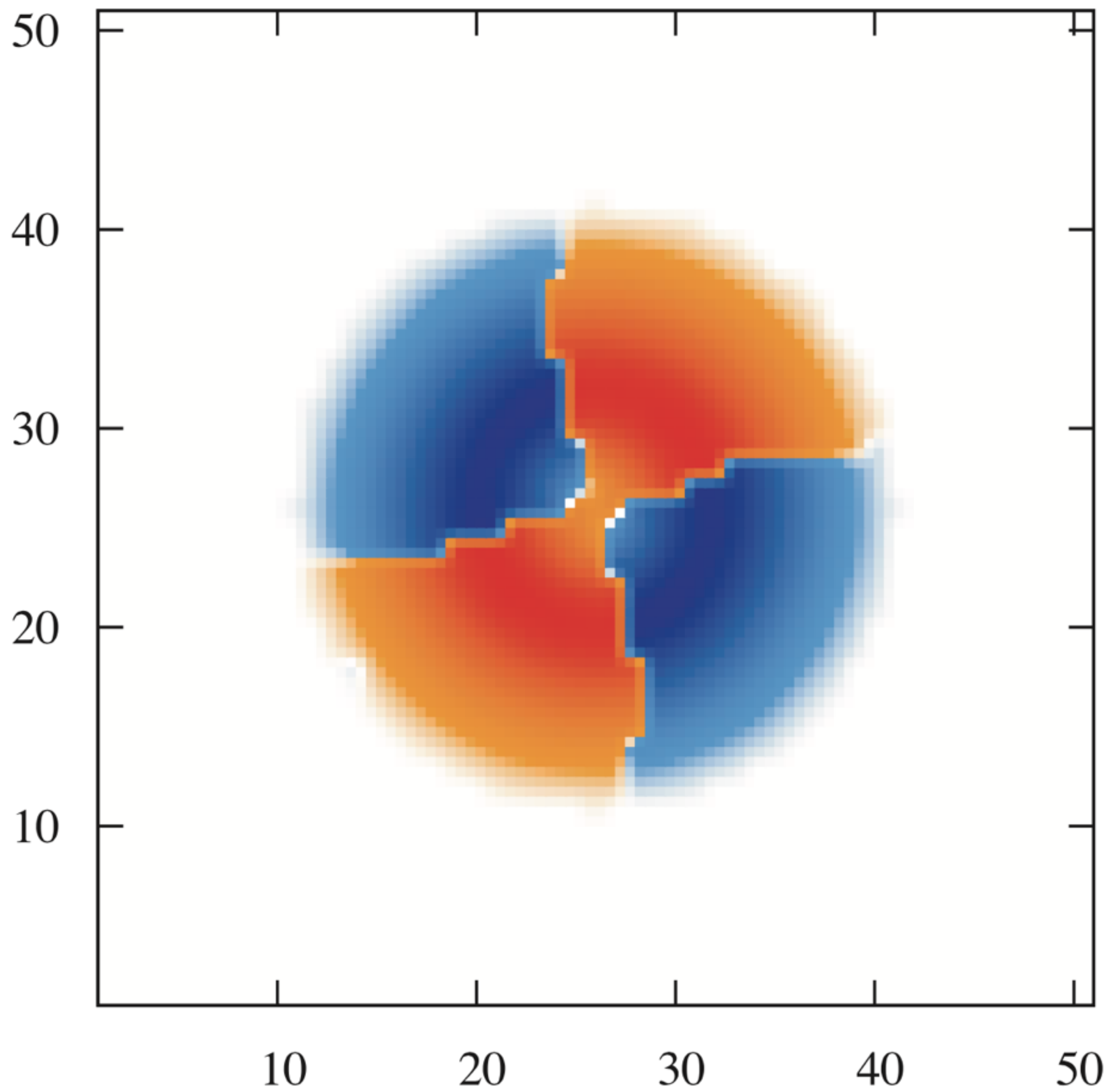

Lattimer-Swesty 220 EOS 1.35+1.35

GRAVITATIONAL WAVE SPECTRUM

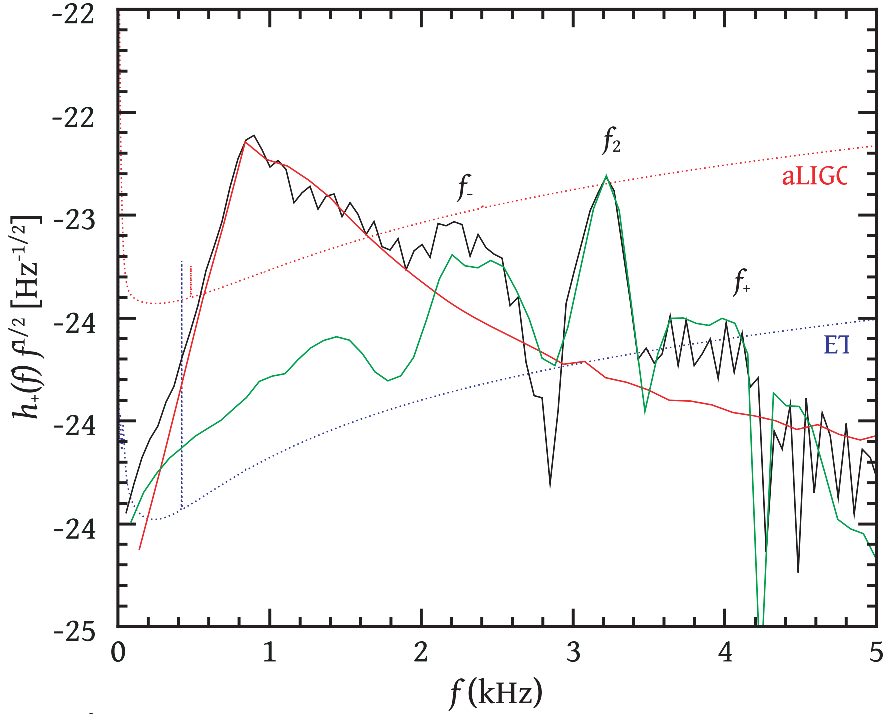

FFT OF HYDRODYNAMICS IN EQUATORIAL PLANE

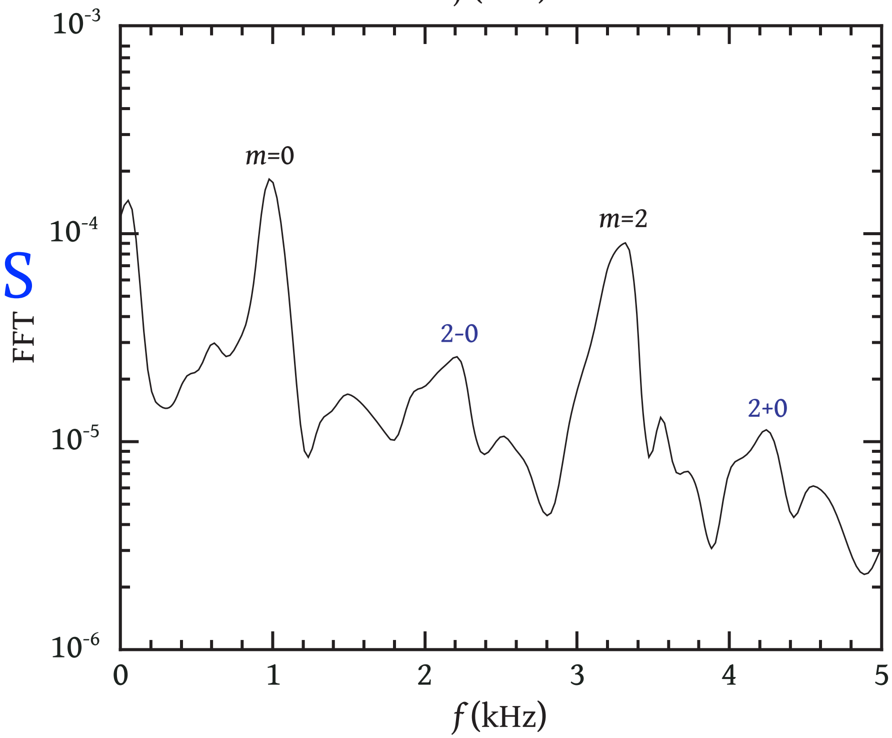

Lattimer-Swesty 220 EOS 1.35+1.35

GRAVITATIONAL WAVE SPECTRUM

FFT OF HYDRODYNAMICS IN EQUATORIAL PLANE

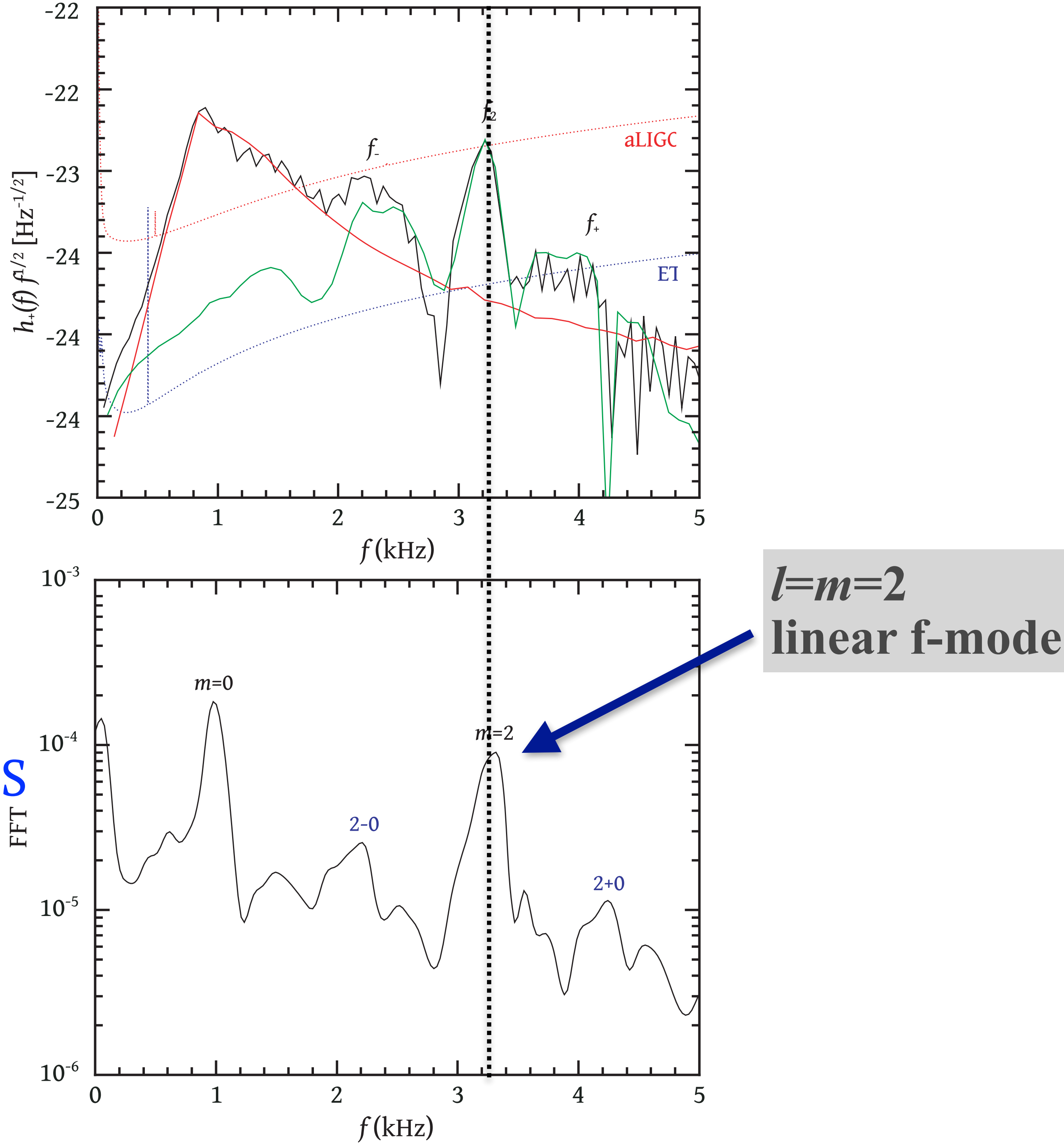

Lattimer-Swesty 220 EOS 1.35+1.35

GRAVITATIONAL WAVE SPECTRUM

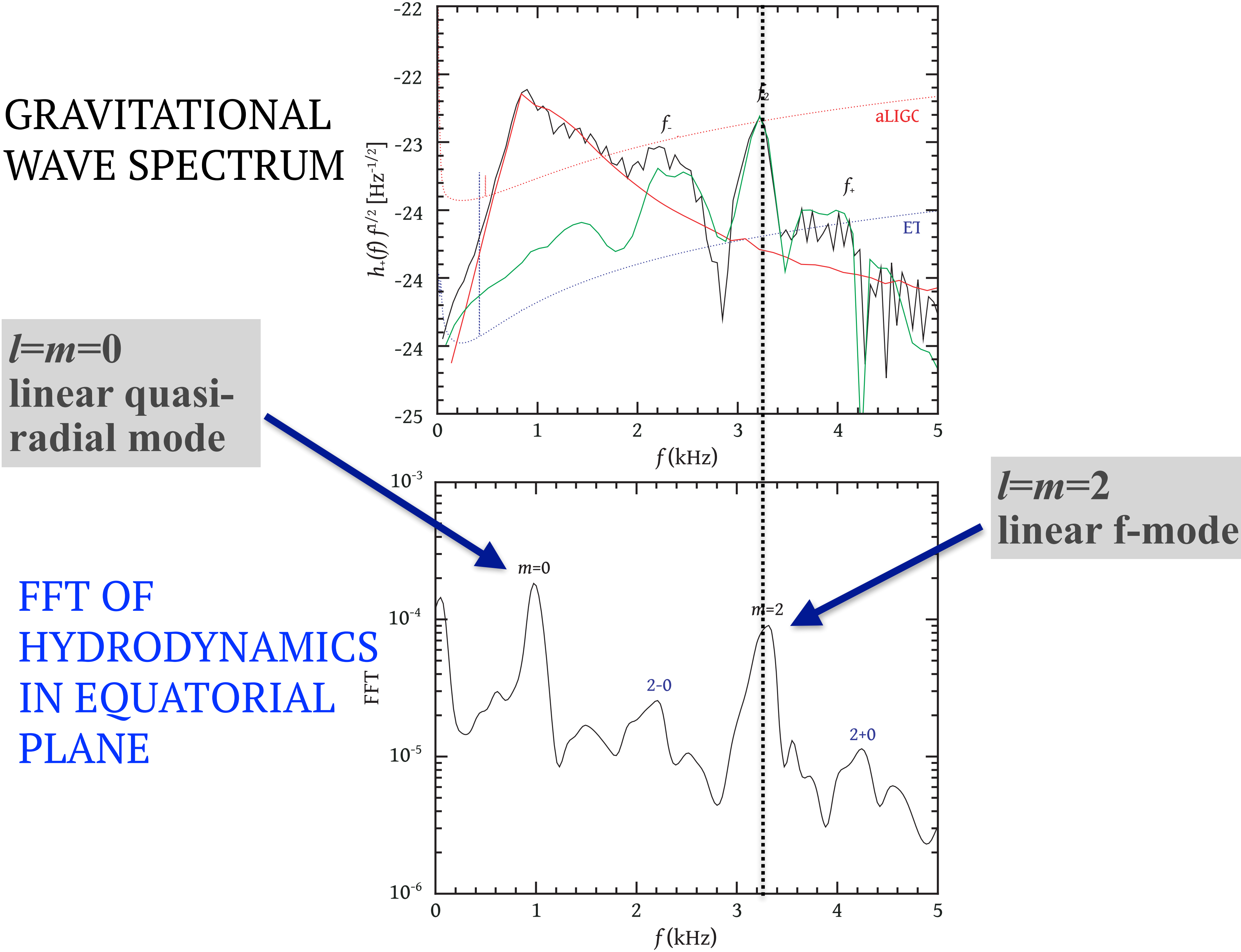

FFT OF HYDRODYNAMICS IN EQUATORIAL PLANE

Lattimer-Swesty 220 EOS 1.35+1.35

GRAVITATIONAL WAVE SPECTRUM

***l=m*=0**
linear quasi-radial mode

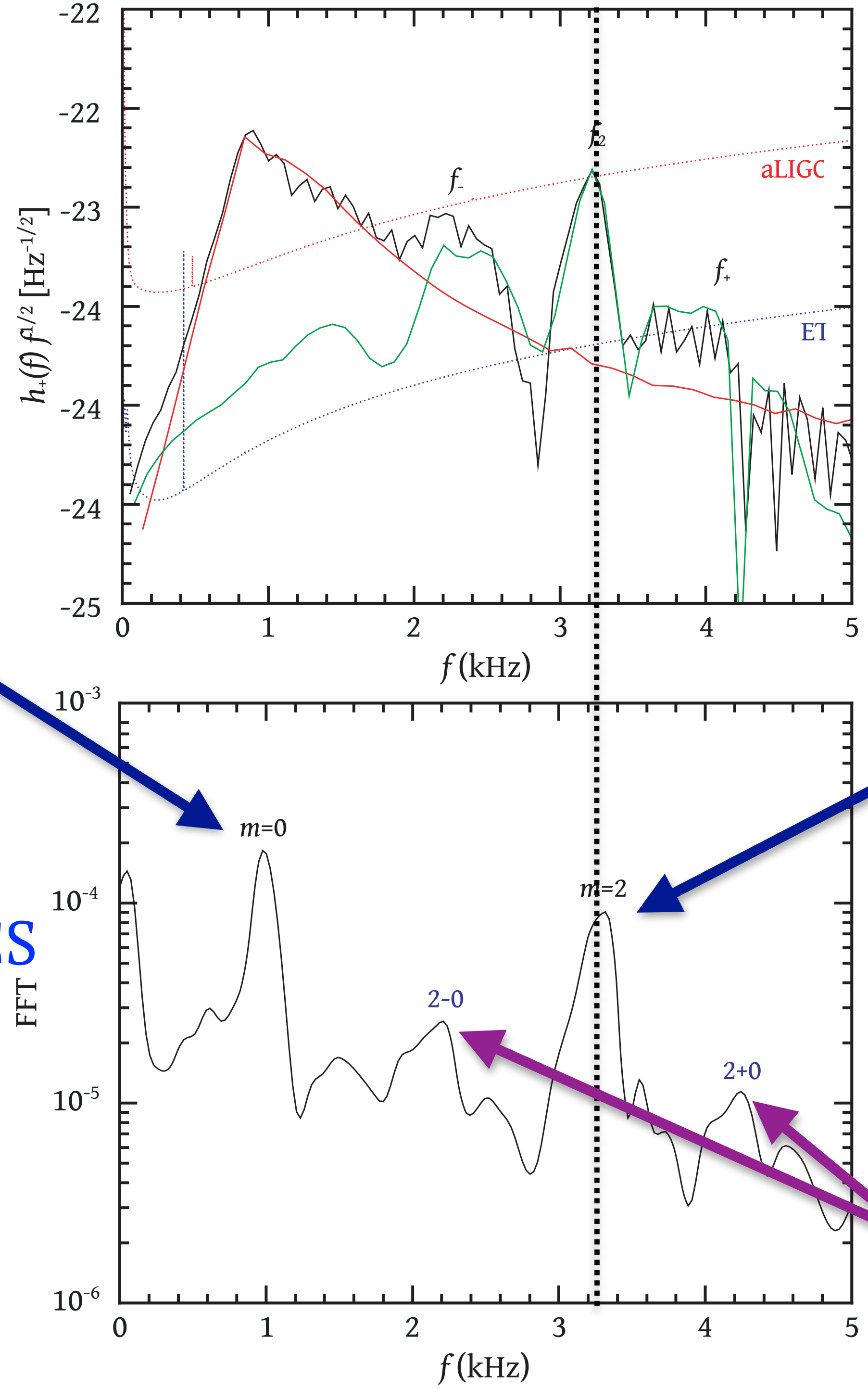

***l=m*=2**
linear f-mode

FFT OF HYDRODYNAMICS IN EQUATORIAL PLANE

"2-0" & "2+0" quasi-linear
combination frequencies

Lattimer-Swesty 220 EOS 1.35+1.35

GRAVITATIONAL WAVE SPECTRUM

$l=m=0$ linear quasi-radial mode

FFT OF HYDRODYNAMICS IN EQUATORIAL PLANE

***"2-0" quasi-linear* combination frequency**

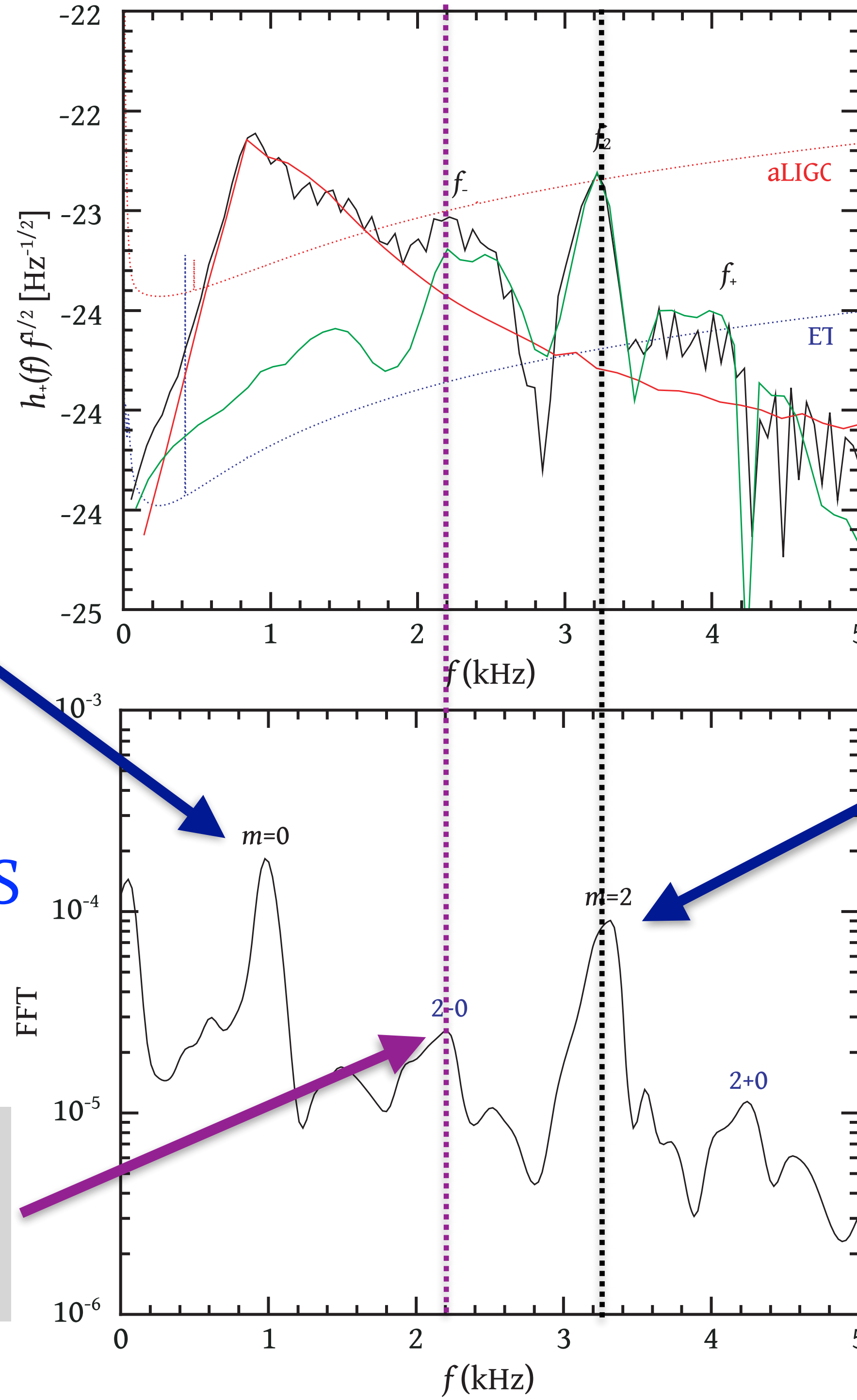

$l=m=2$ linear f-mode

Tracing Individual Particles

Using SPH it is simple to trace the paths of particles that originally belonged to one or the other star

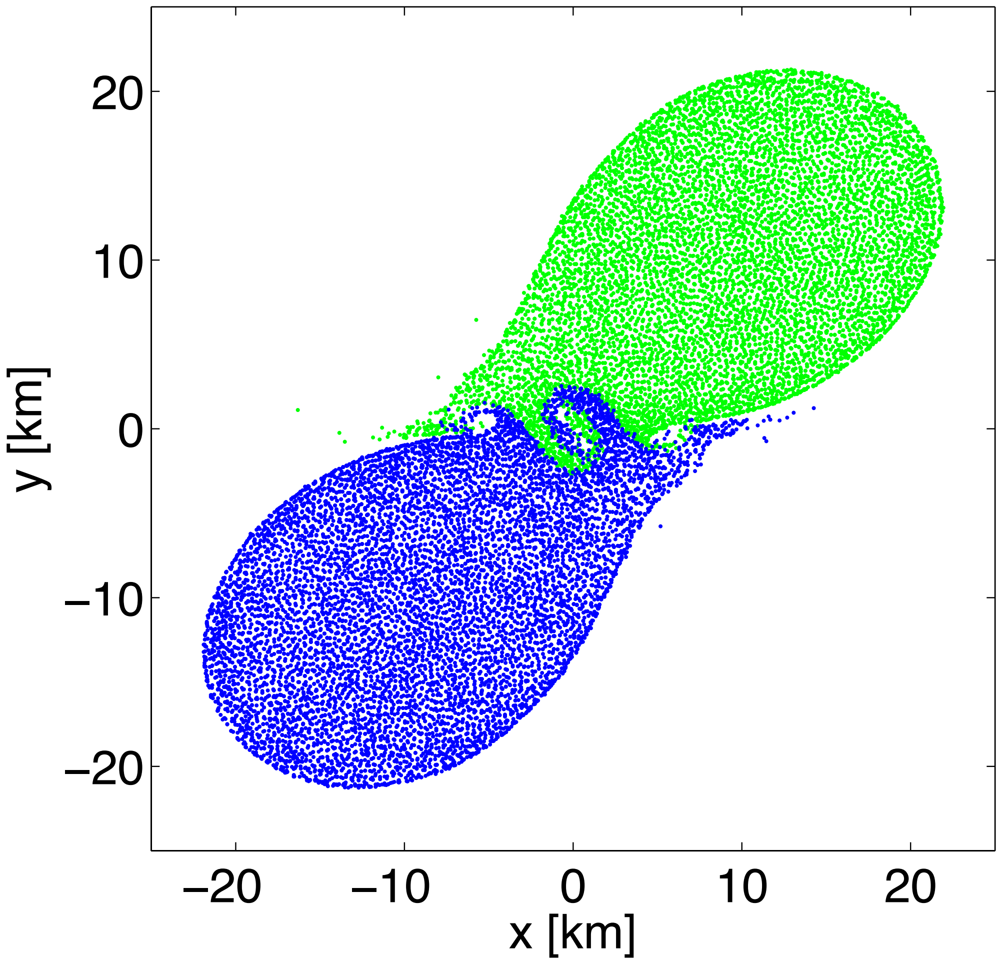

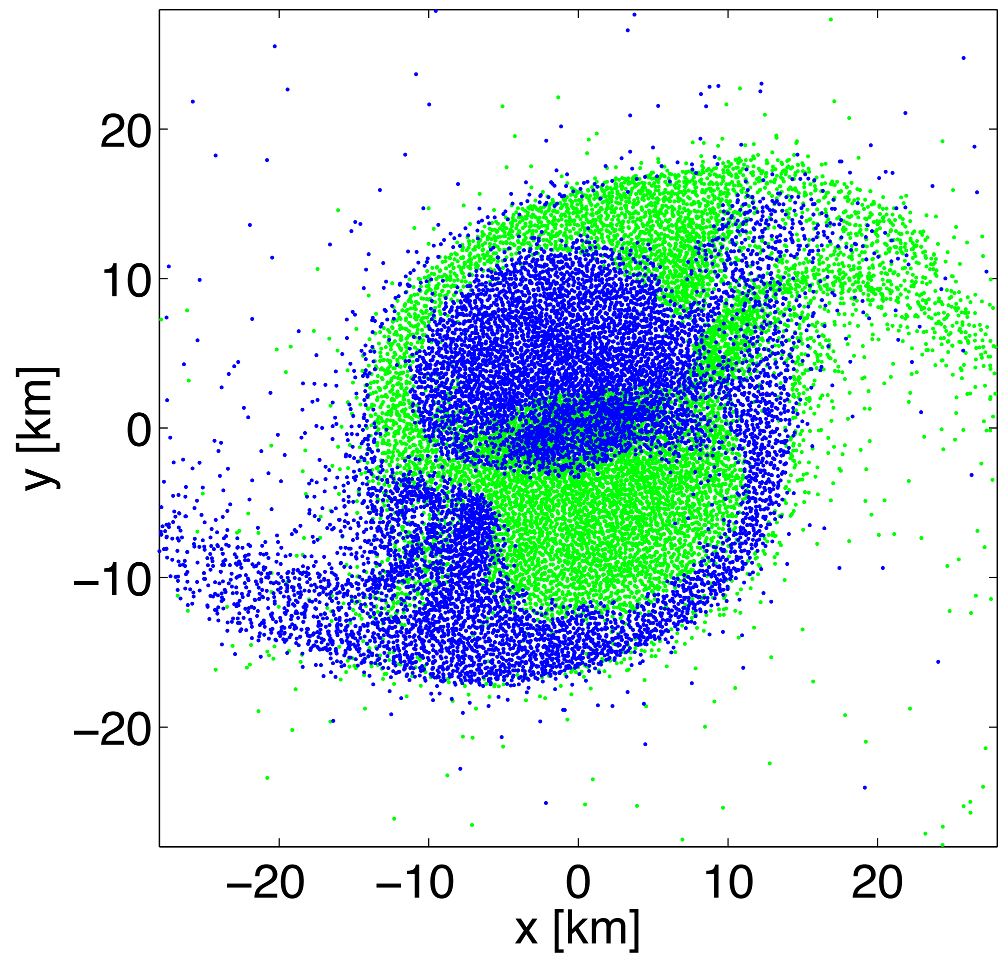

Spiral Deformation

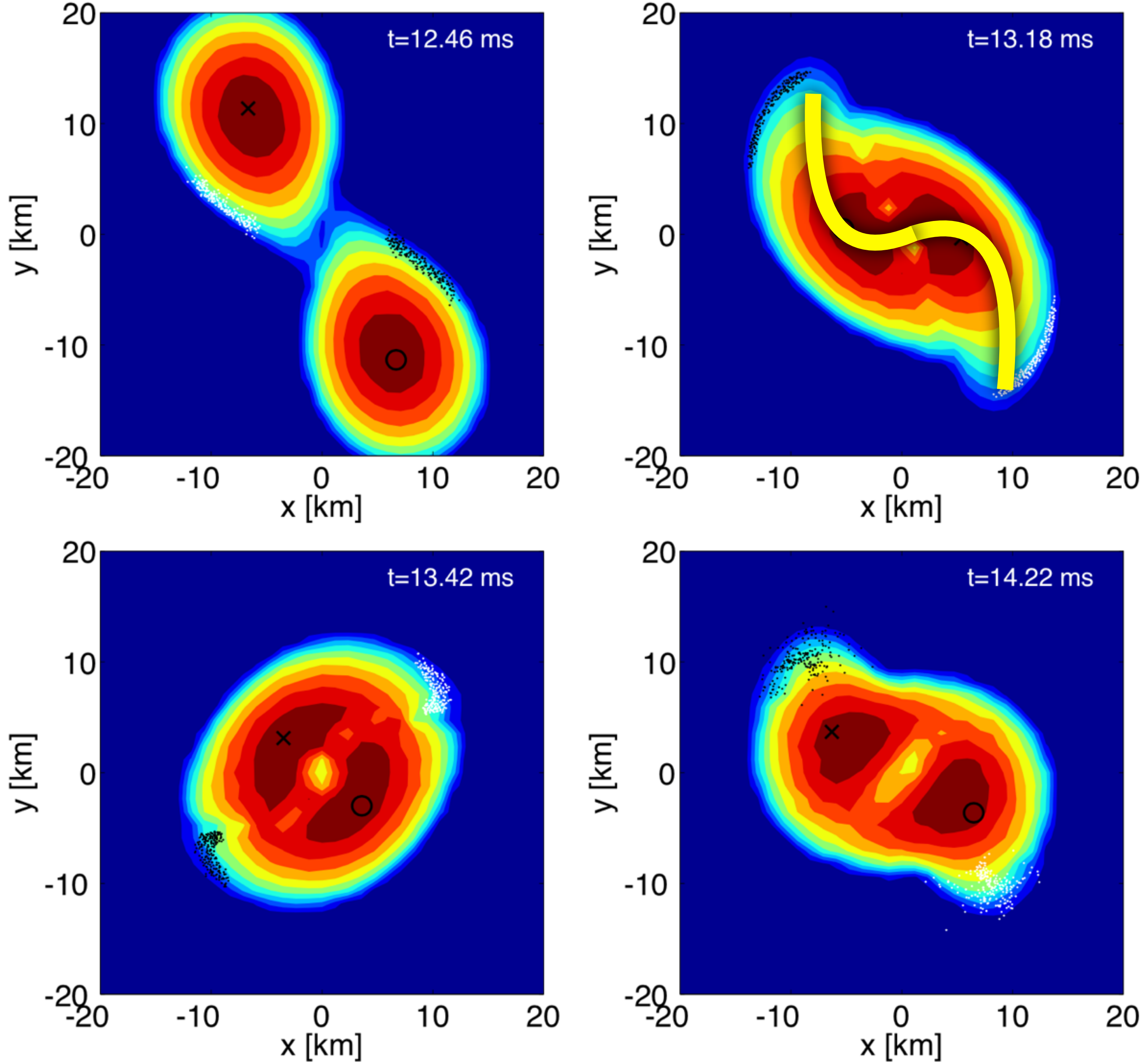

Lattimer-Swesty 220 EOS 1.35+1.35

GRAVITATIONAL WAVE SPECTRUM

$l=m=0$
linear quasi-radial mode

FFT OF HYDRODYNAMICS IN EQUATORIAL PLANE

"2-0" quasi-linear
combination frequency

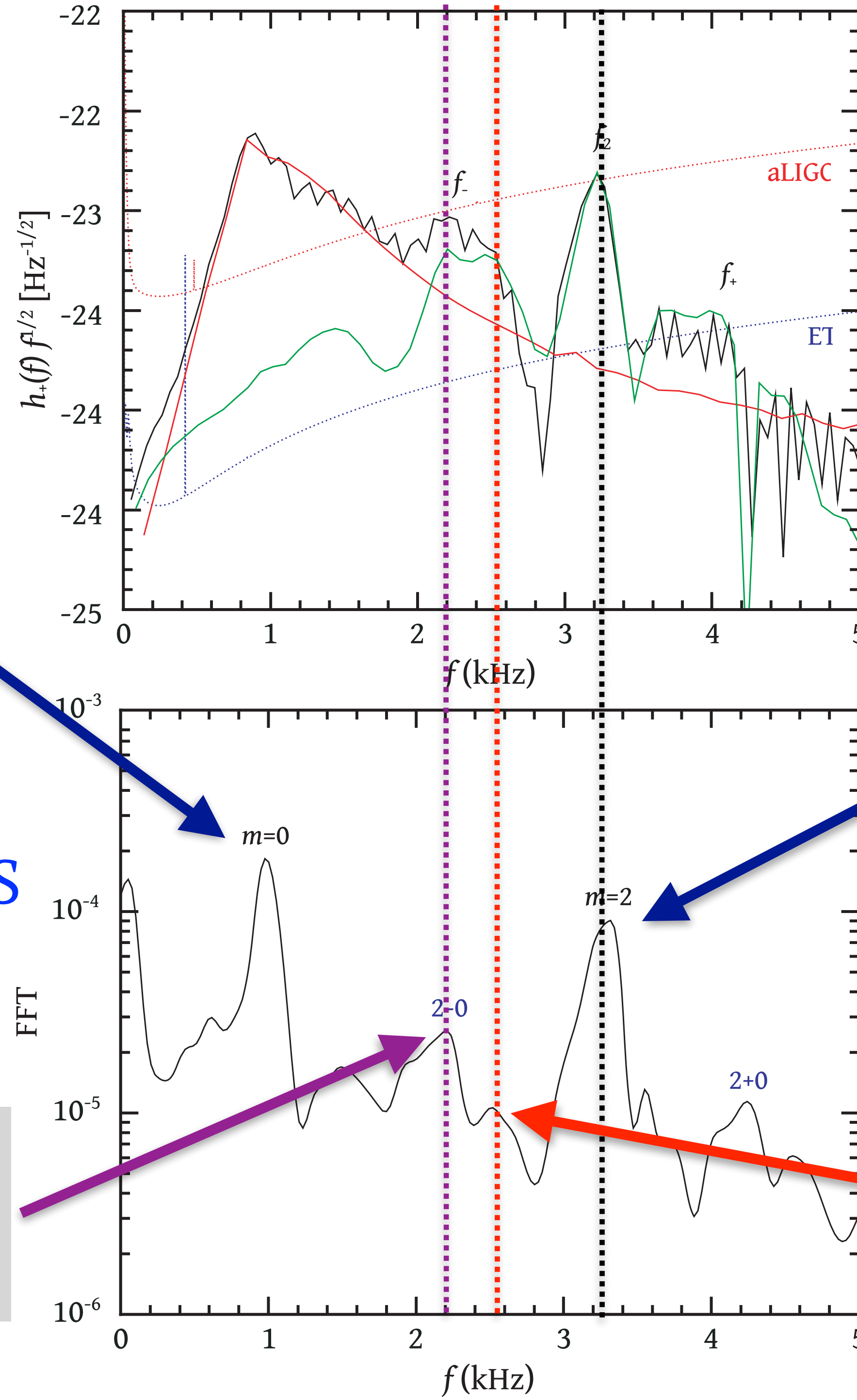

$l=m=2$
linear f-mode

nonlinear
spiral frequency

Lattimer-Swesty 220 EOS 1.35+1.35

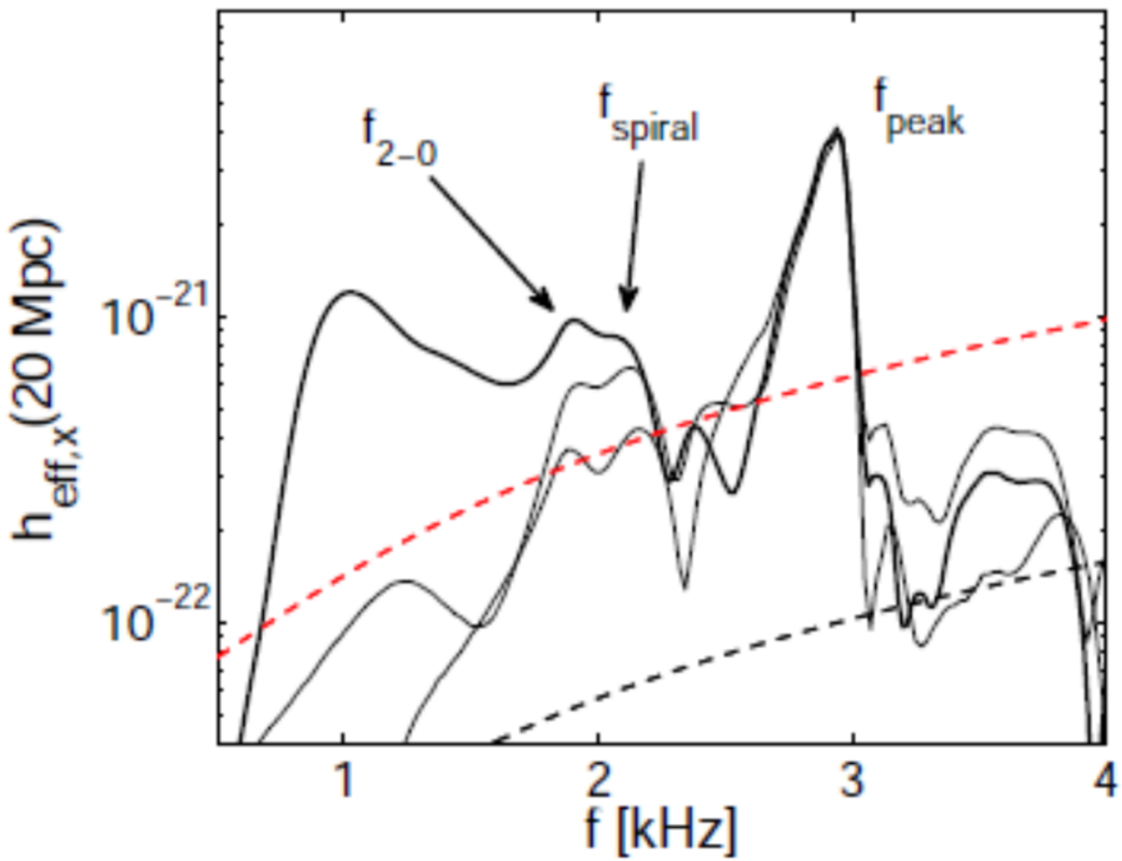

Linear l=m=2 f_{peak} remains nearly constant in time.

Quasi-linear "2-0" and nonlinear f_{spiral} decay with time, as expected.

DD2 EOS 1.35+1.35

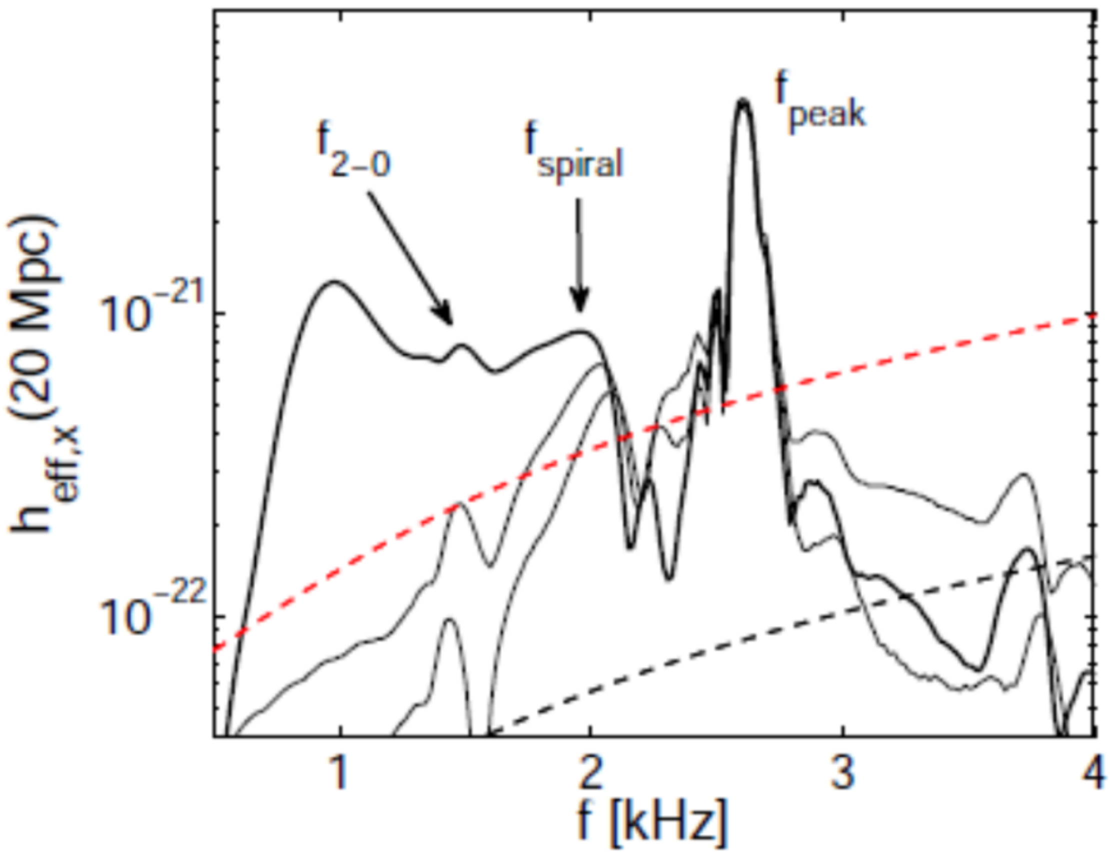

Linear *l*=*m*=2 $f_{\mathbf{peak}}$ remains nearly constant in time.

Quasi-linear “2-0” and nonlinear $f_{\mathbf{spiral}}$ decay with time, as expected.

NL3 EOS 1.35+1.35

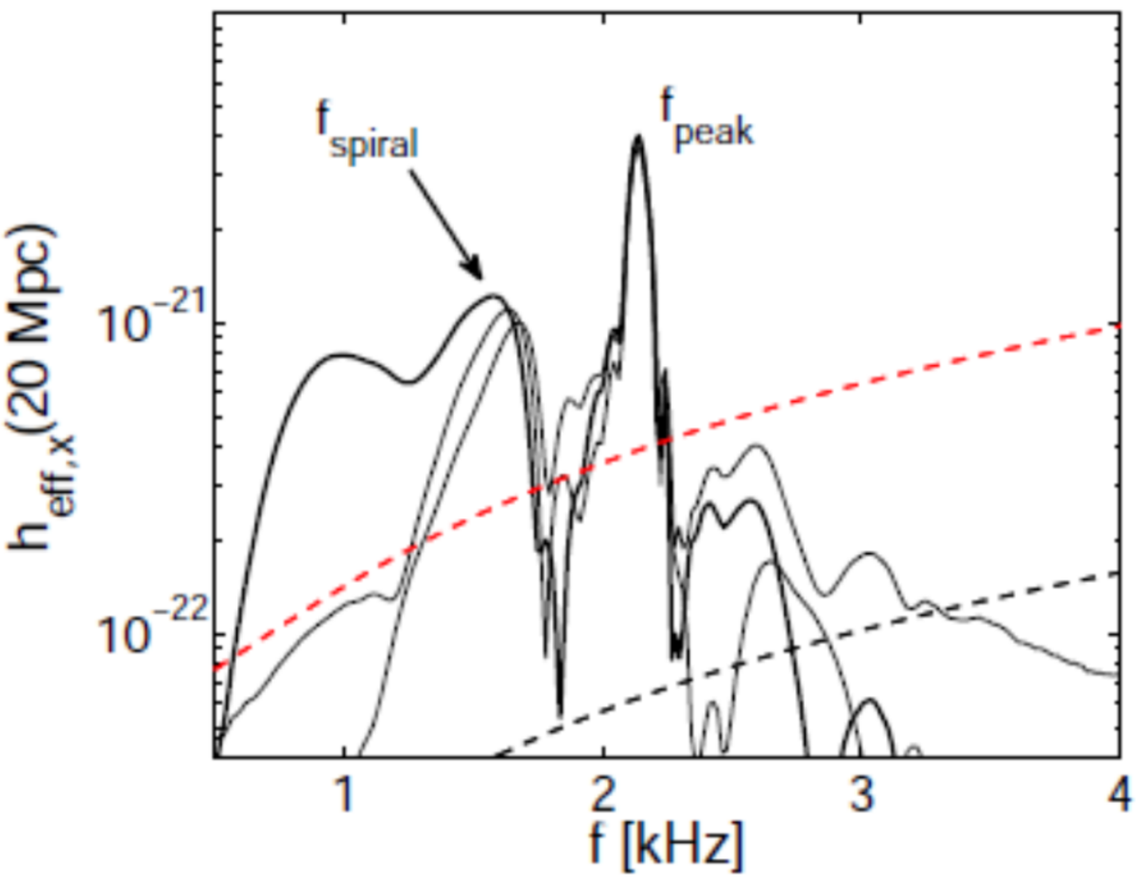

Linear l=m=2 $\boldsymbol{f}_{\mathbf{peak}}$ remains nearly constant in time.

Quasi-linear "2-0" and nonlinear $\boldsymbol{f}_{\mathbf{spiral}}$ decay with time, as expected.

Three Types of Post-Merger Dynamics

Bauswein, NS (2015)

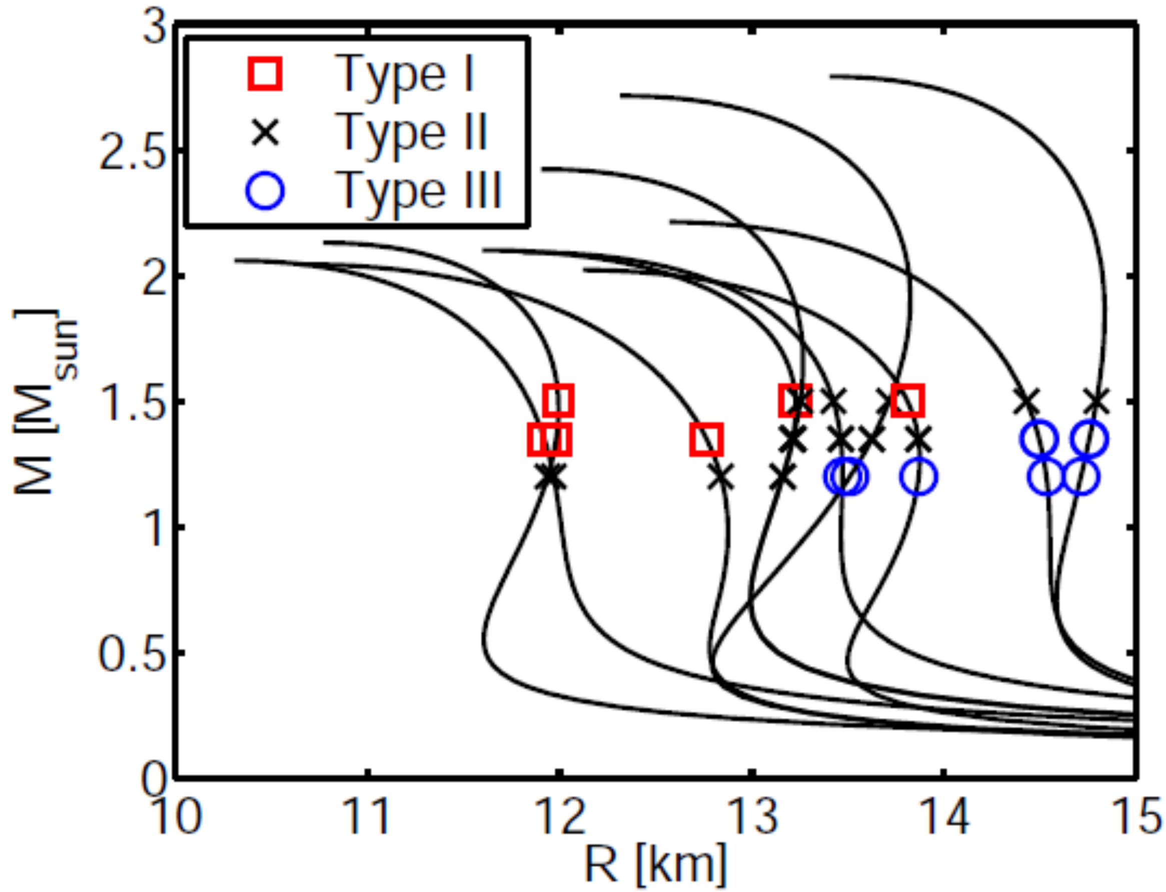

Type I: the “2-0” combination frequency dominates

Type II: **both** the “2-0” and the f_spiral frequencies are present

Type III: the f_spiral frequency dominates

Different Behavior of the Lapse Function

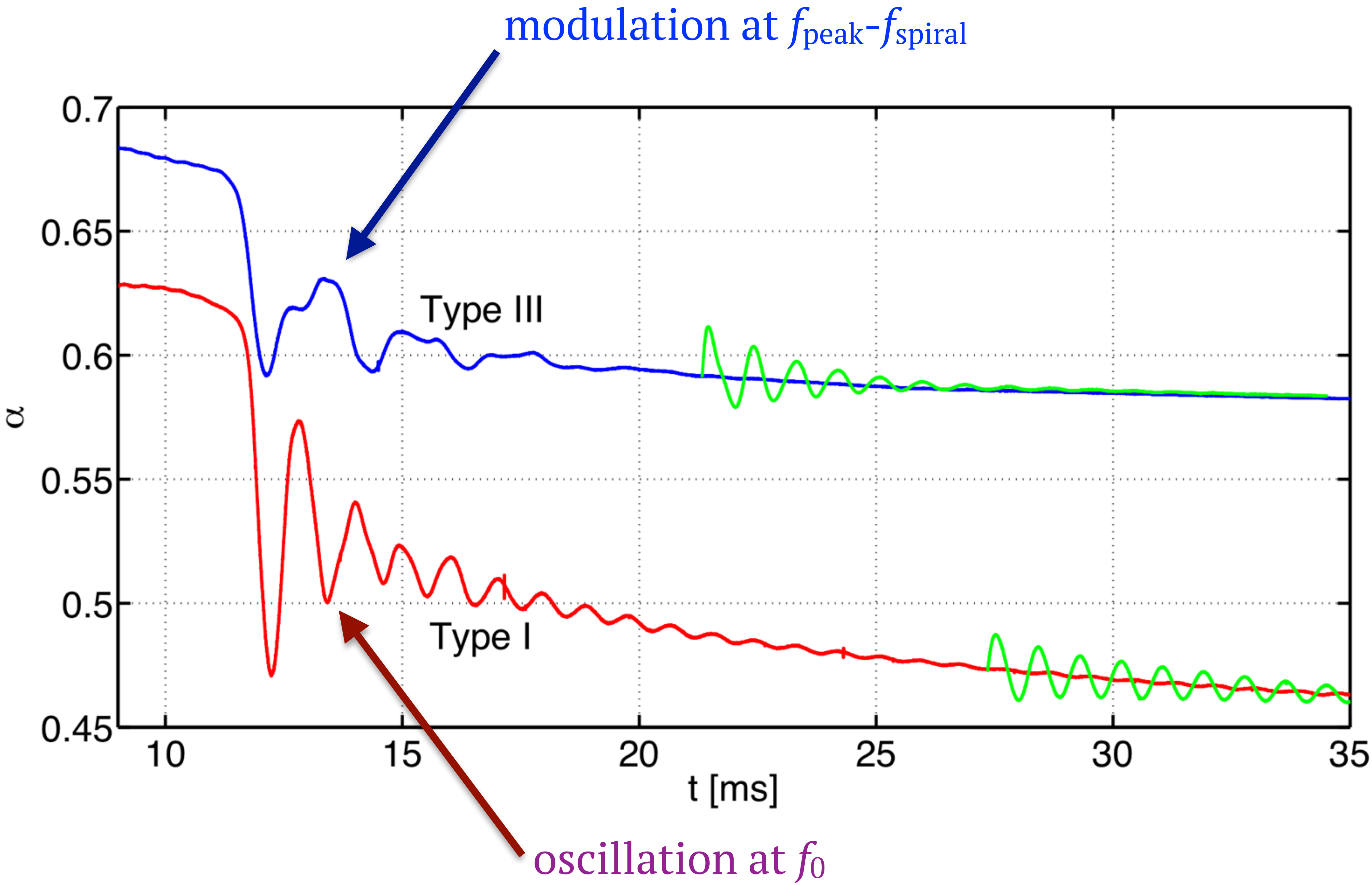

Radius Determination from Post-Merger Signal

Bauswein, Janka, Hebeler & Schwenk (2012)

f_{peak} correlates very well with the radius @ 1.6 Msun, if M_{tot} is known from inspiral.

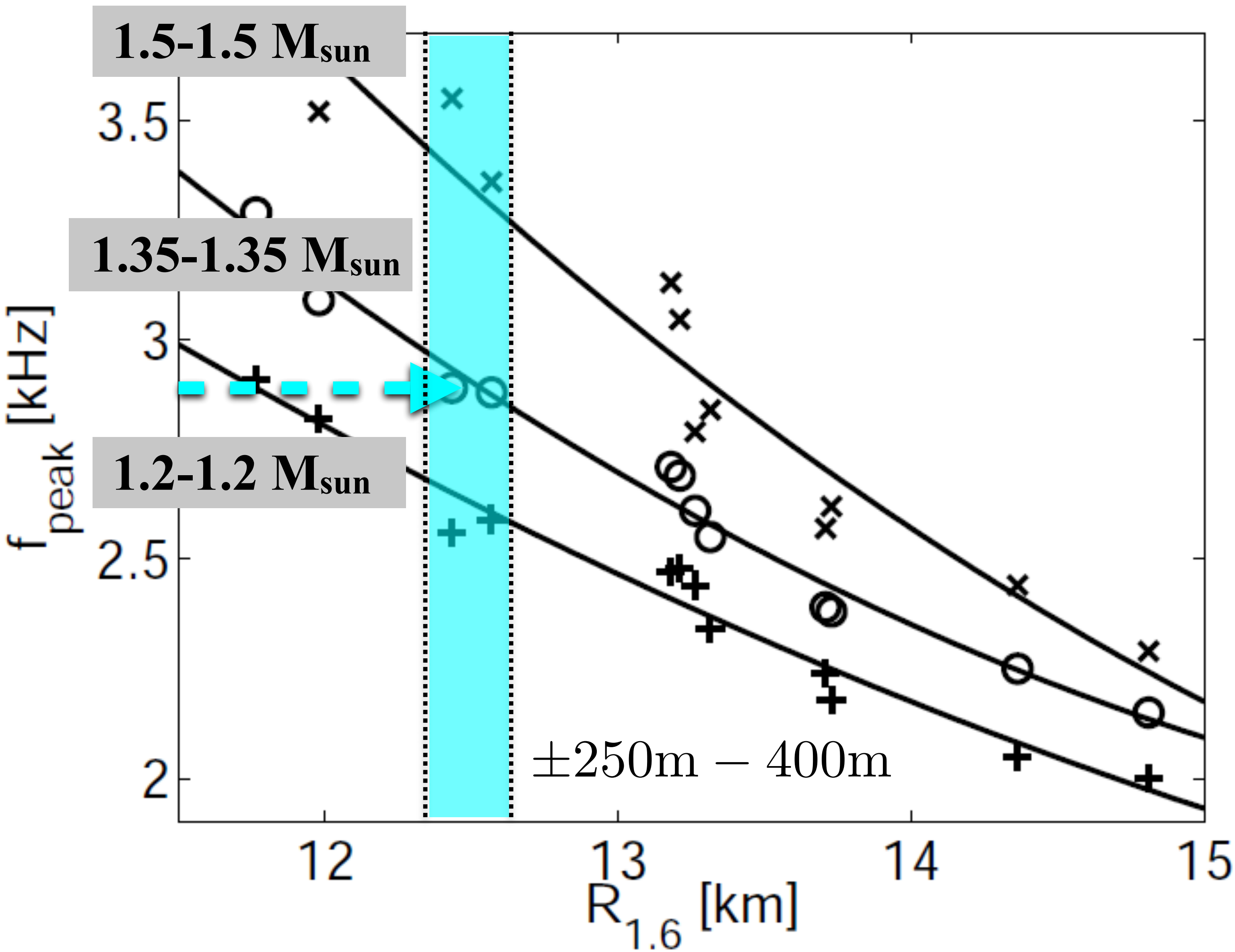

f_{spiral} vs. Compactness

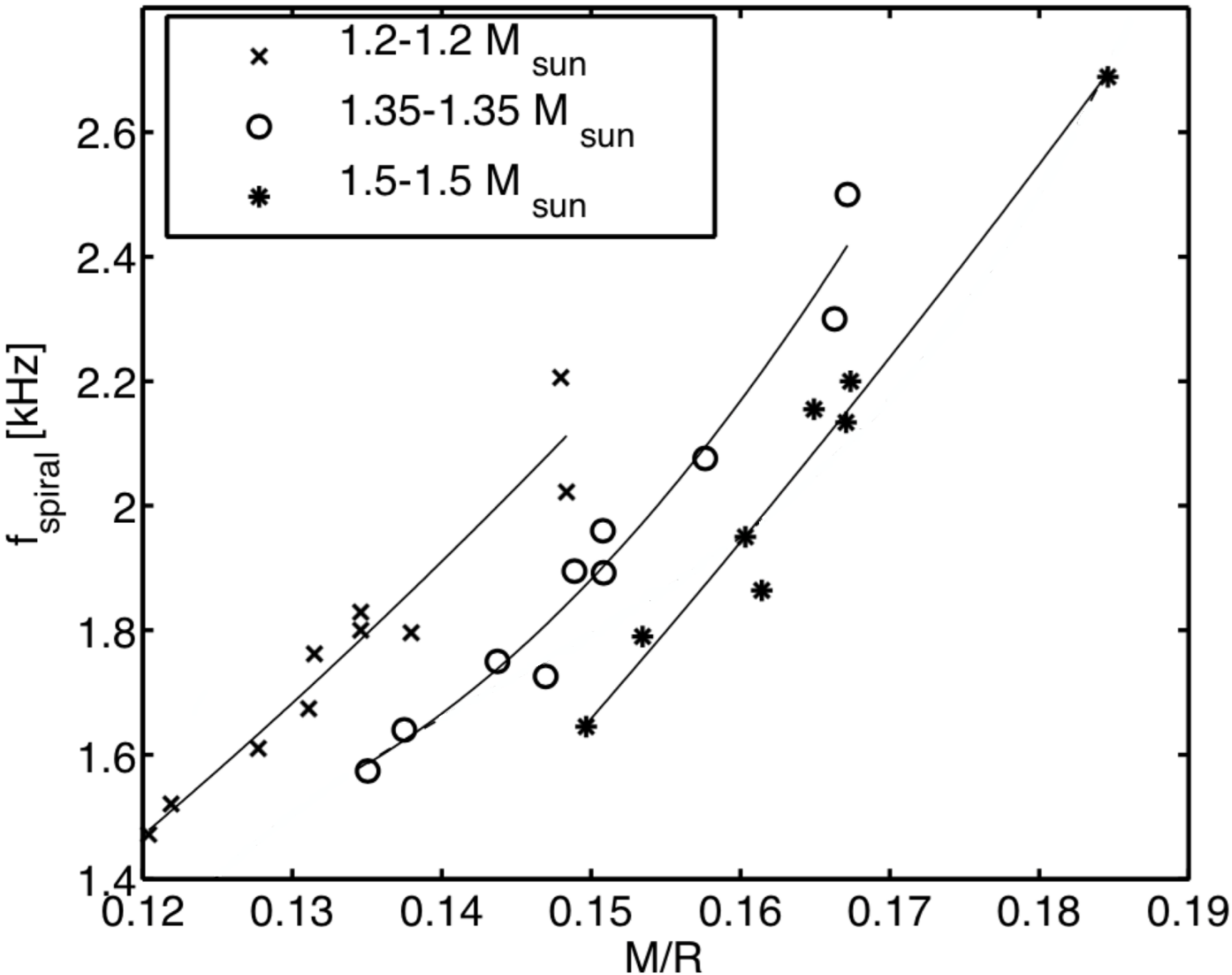

Takami et al. (2015) “universal” relation

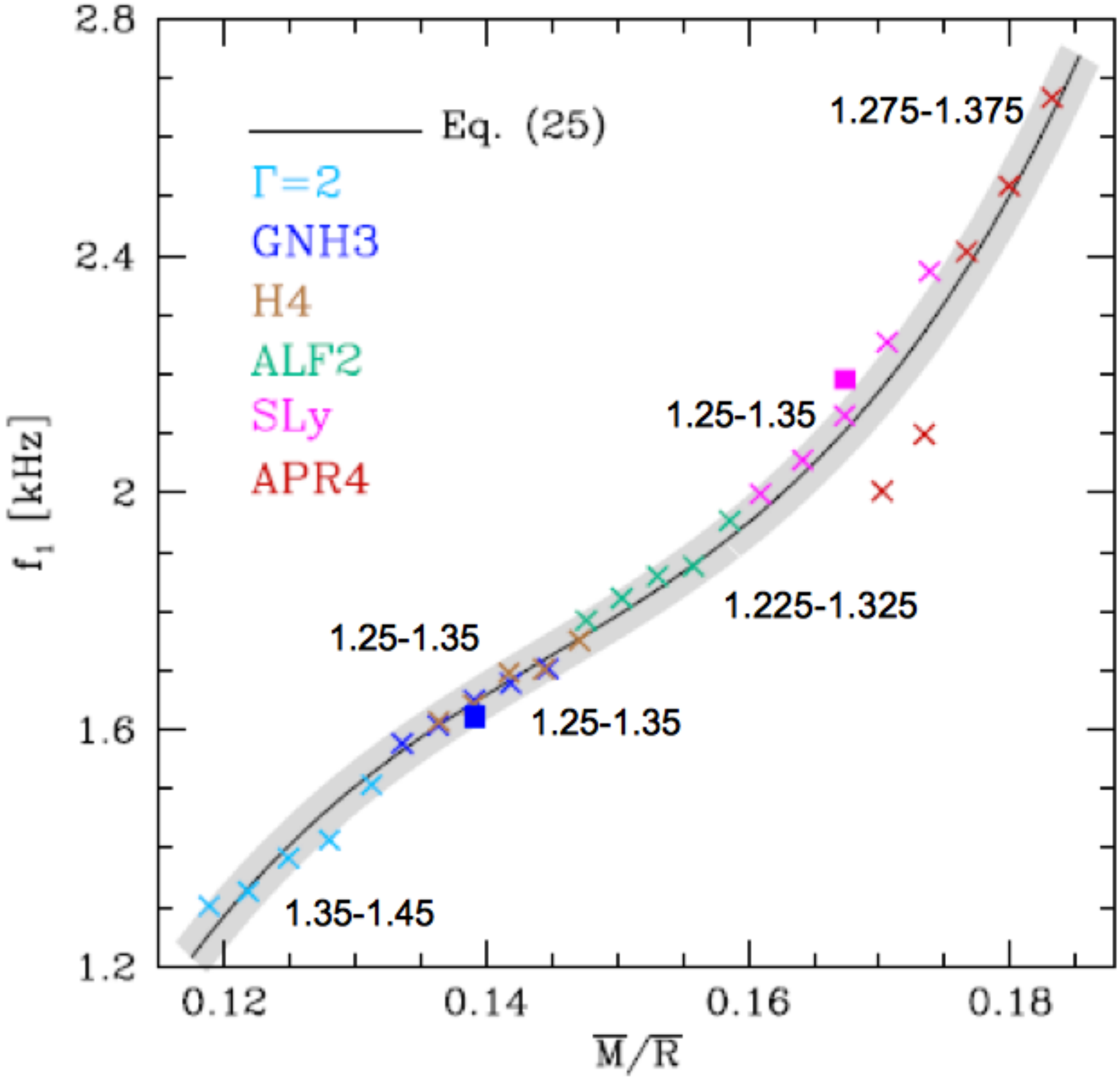

f_{spiral} vs. Compactness

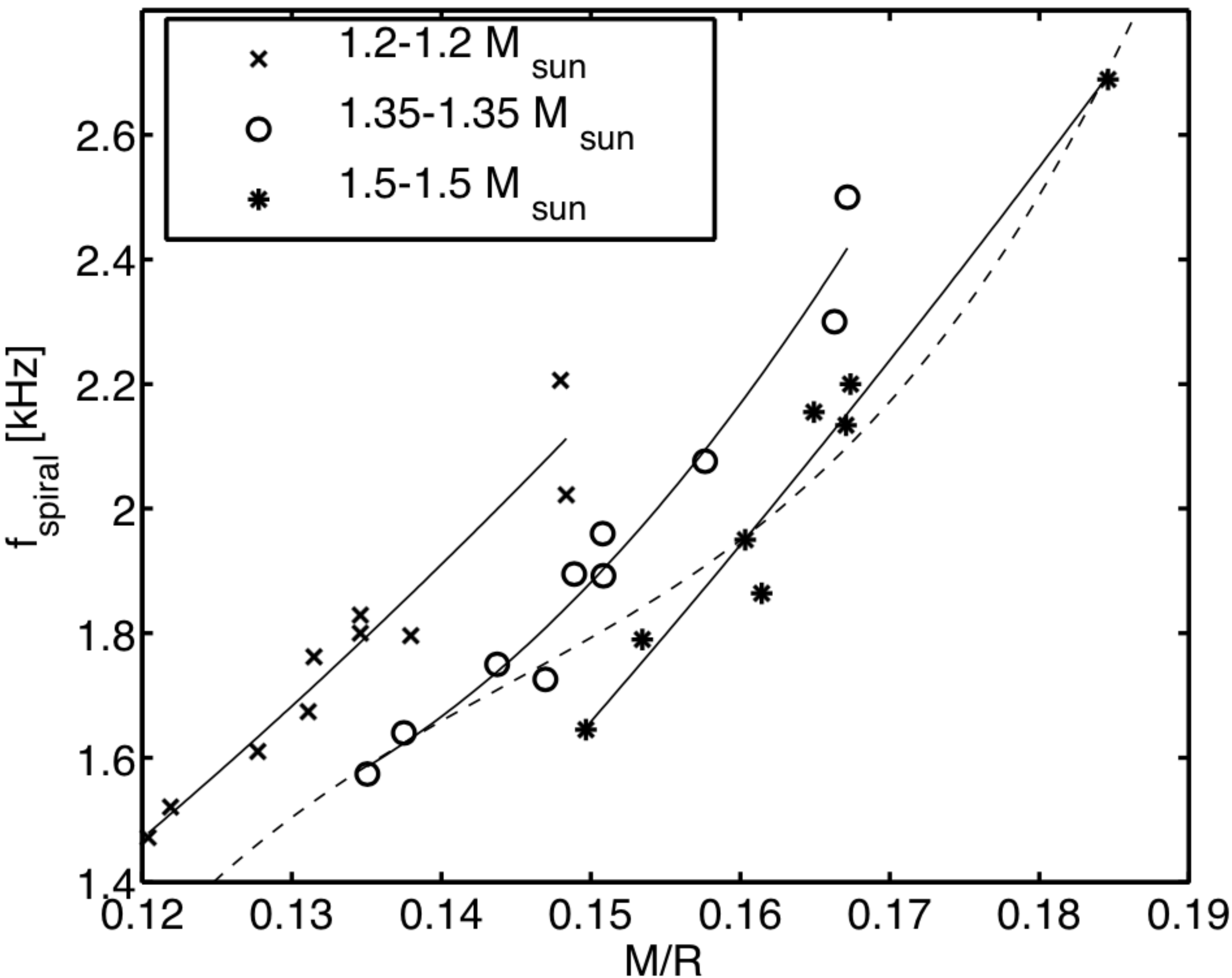

$f_{2\text{-}0}$ vs. Compactness

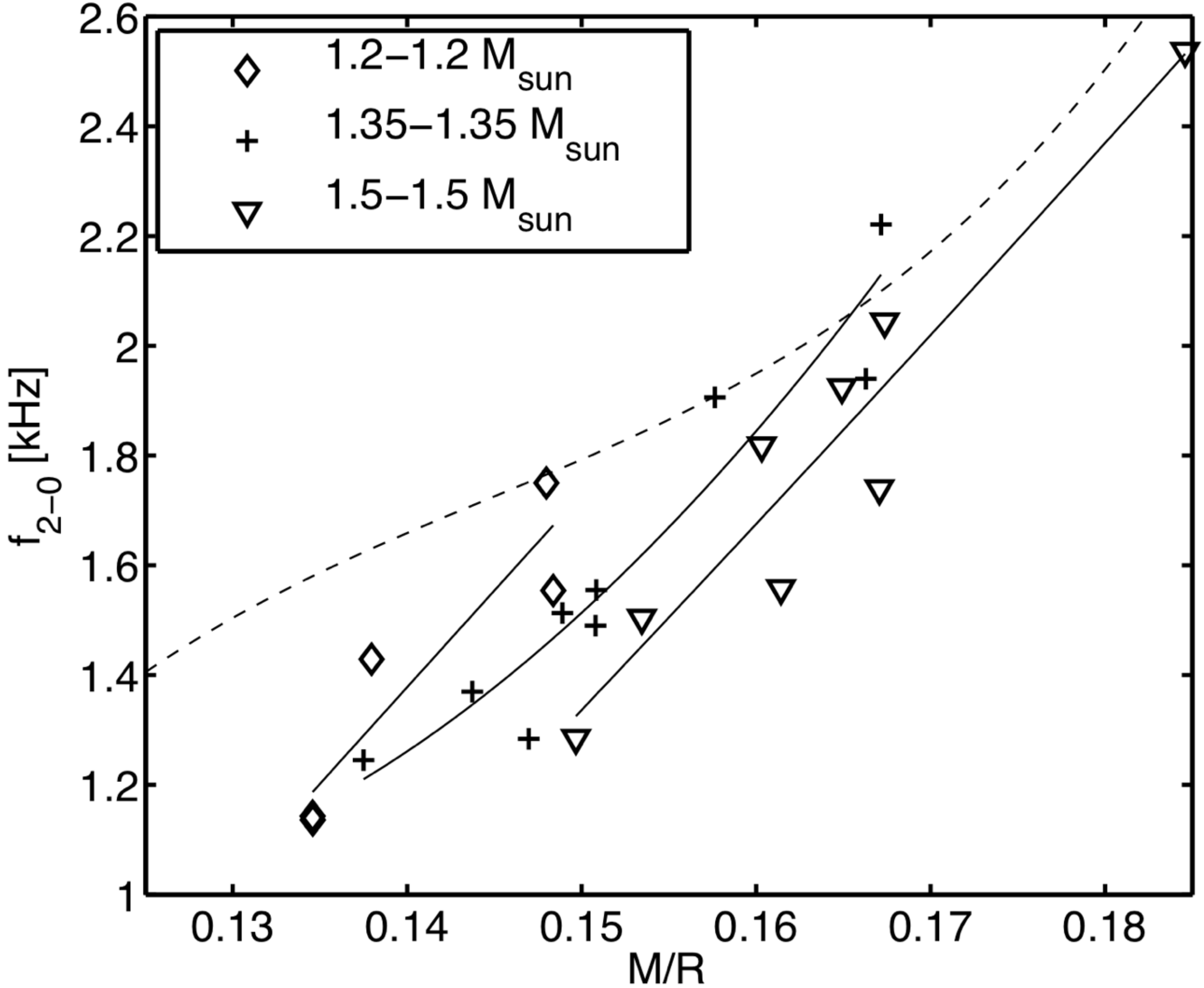

Revealing the EOS

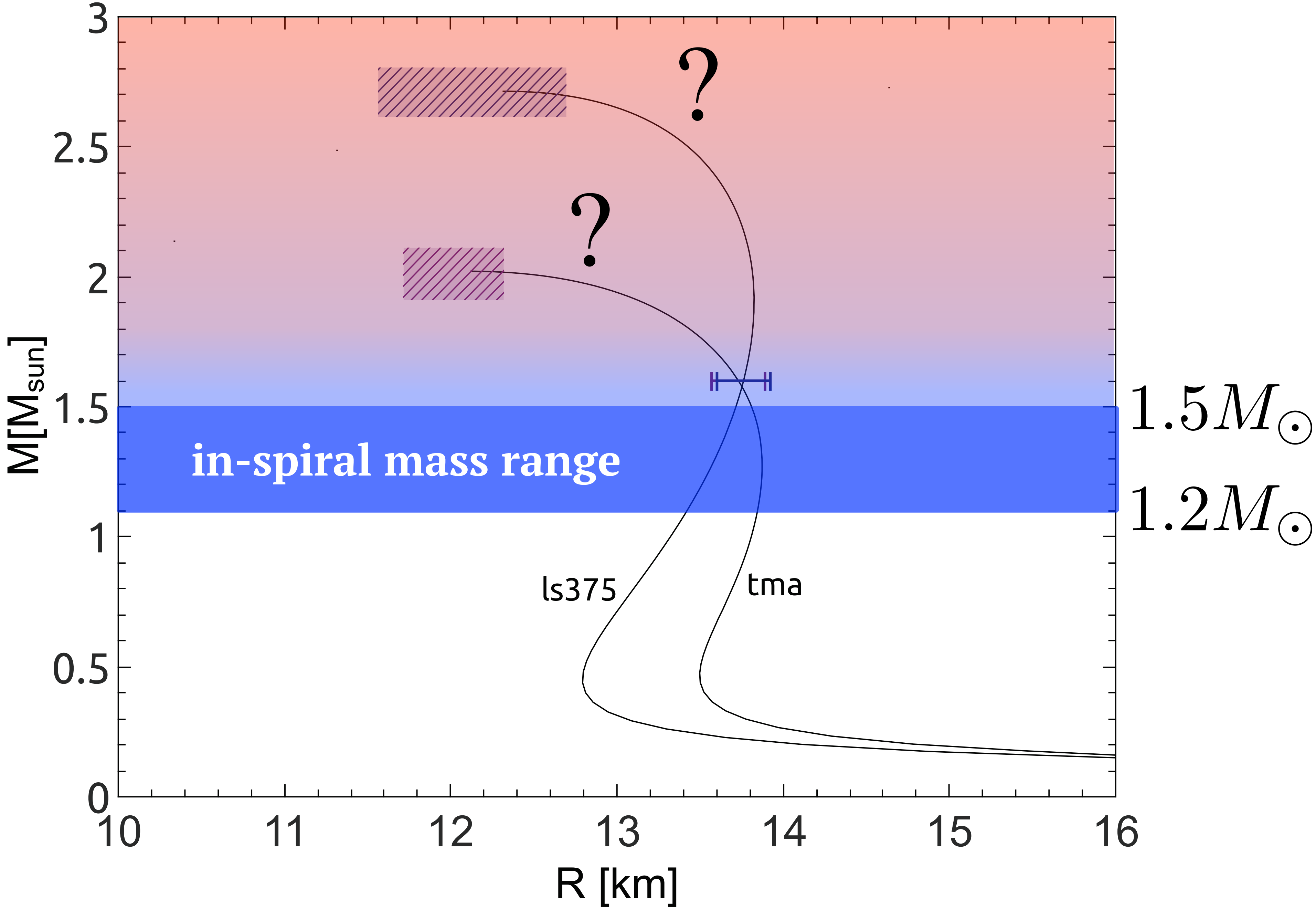

Breaking the EOS Degeneracy

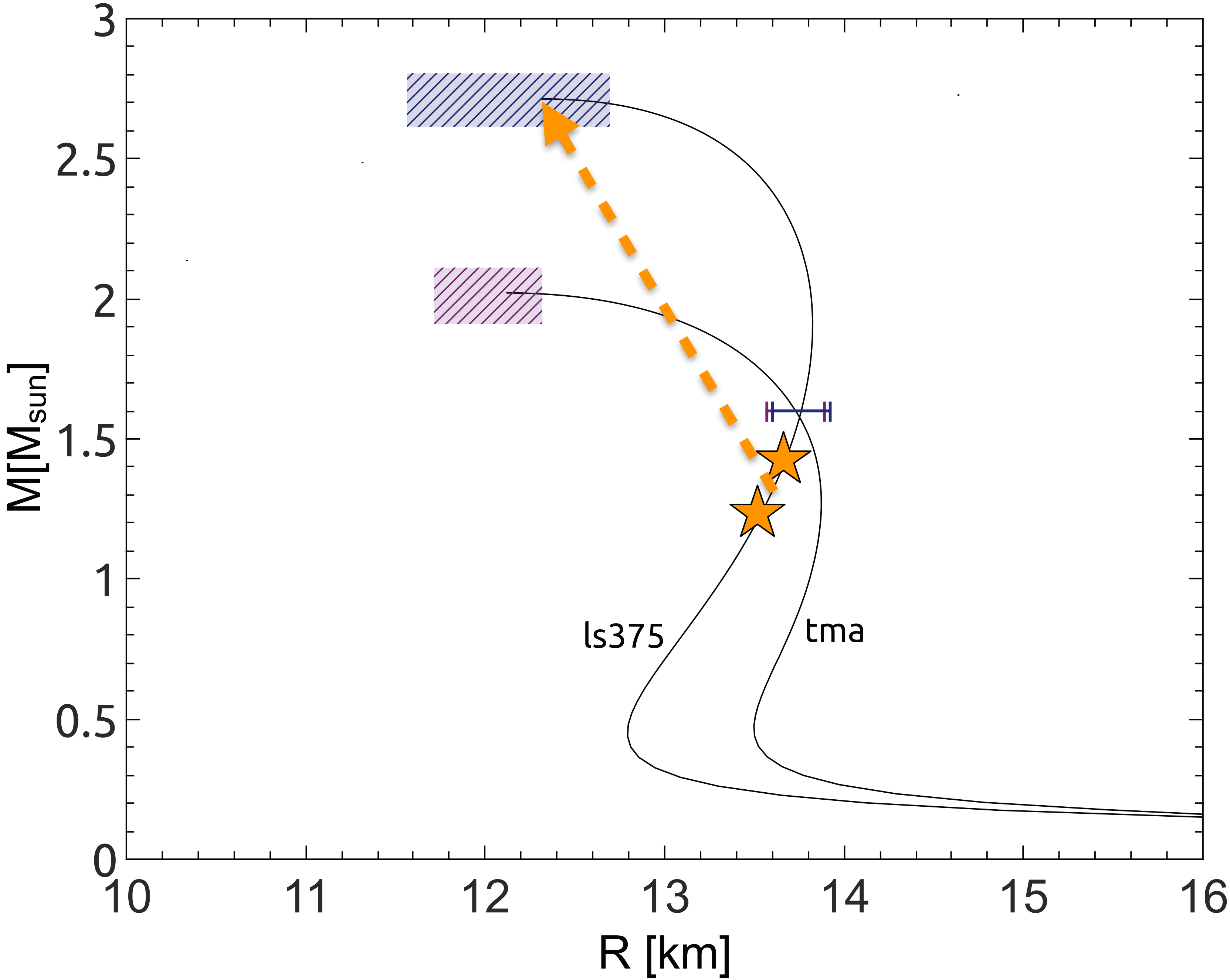

Extrapolating to Larger Masses

Bauswein, NS, Janka (2014)

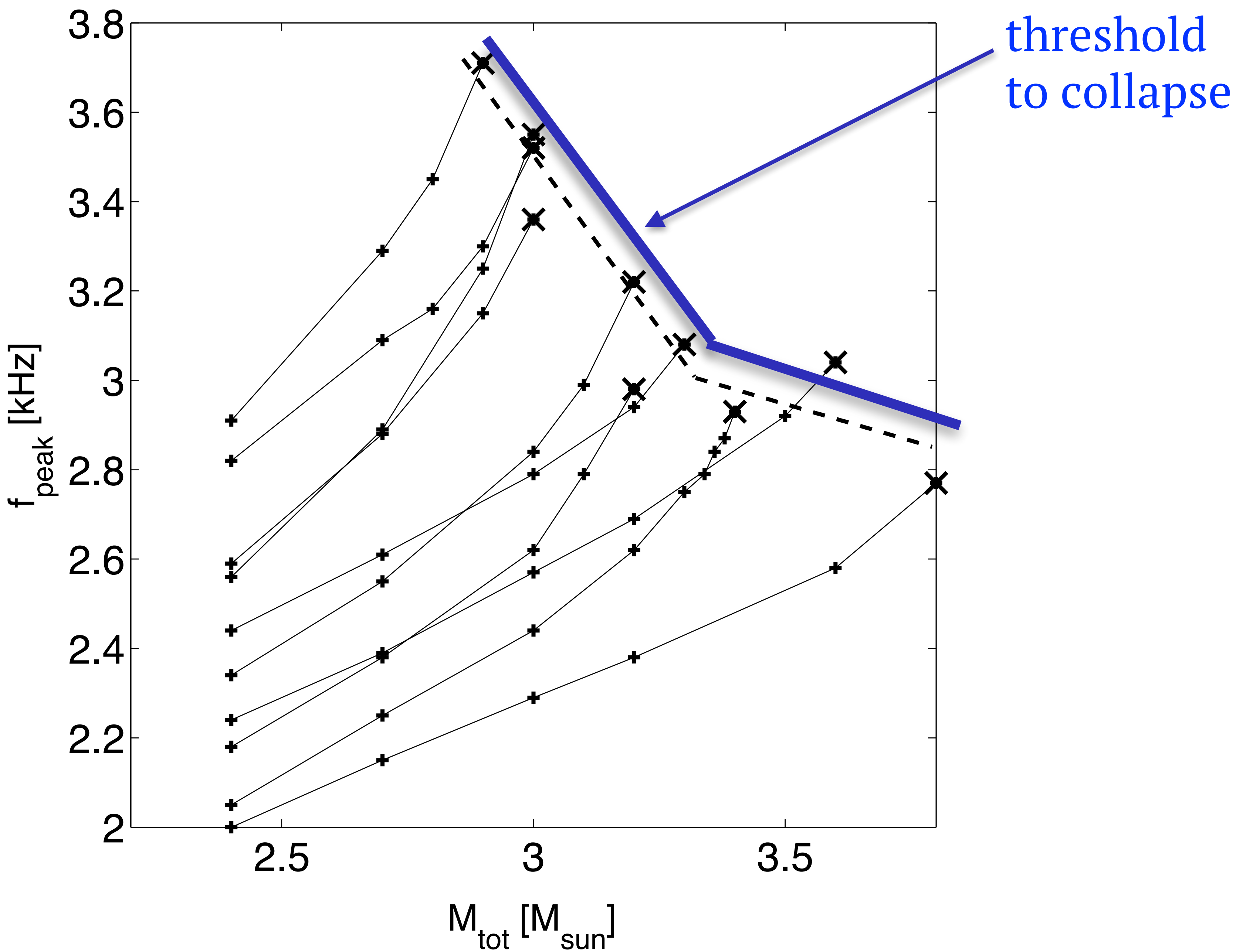

Extrapolating to Larger Masses

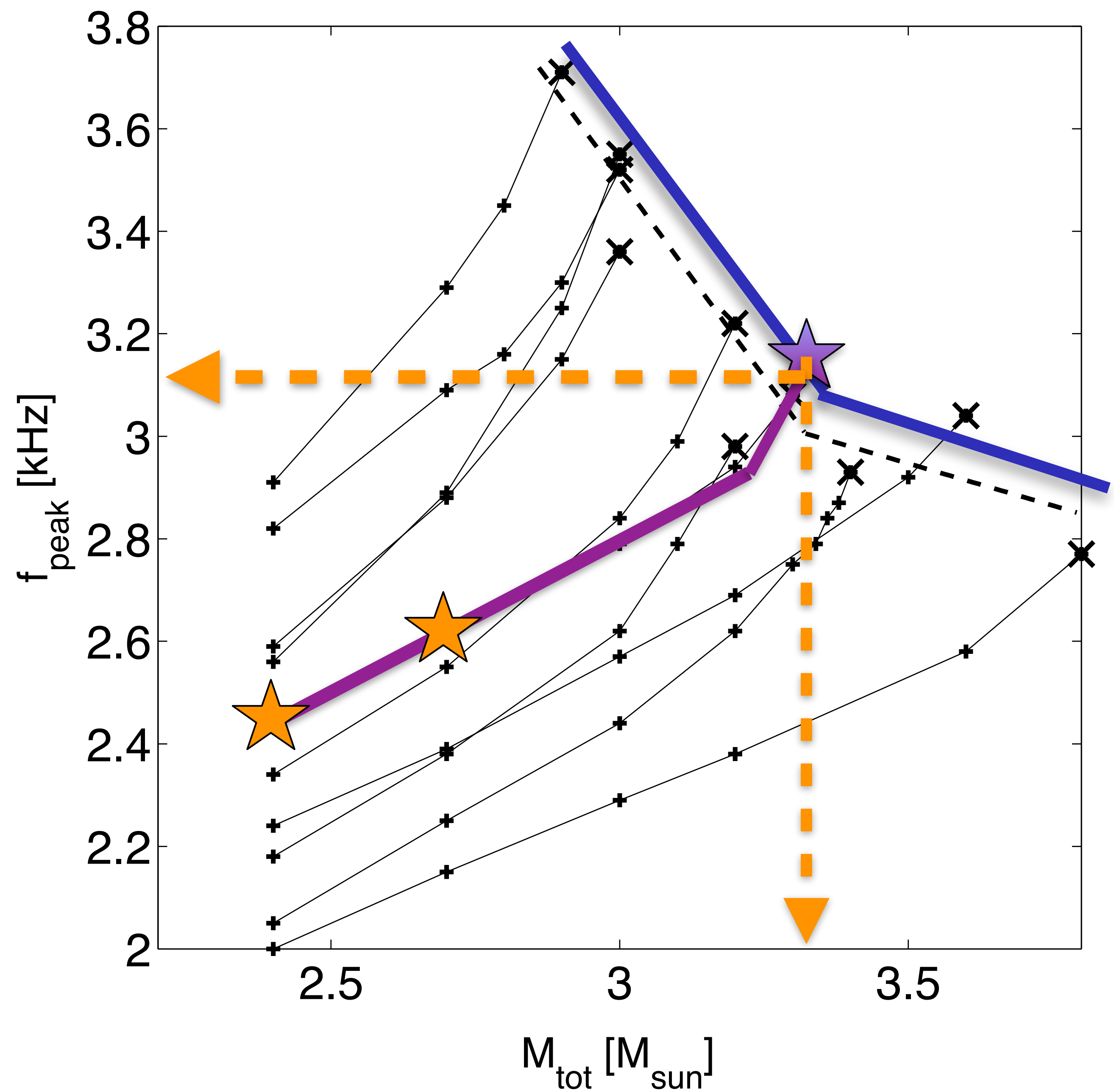

M_thres vs. M_max correlation

Bauswein, Baumgarte, Janka PRL (2013)

The threshold mass is related to the maximum TOV mass as

$$M_{\rm thres} = k \cdot M_{\rm max}$$

where *k* is dependent on the compactness.

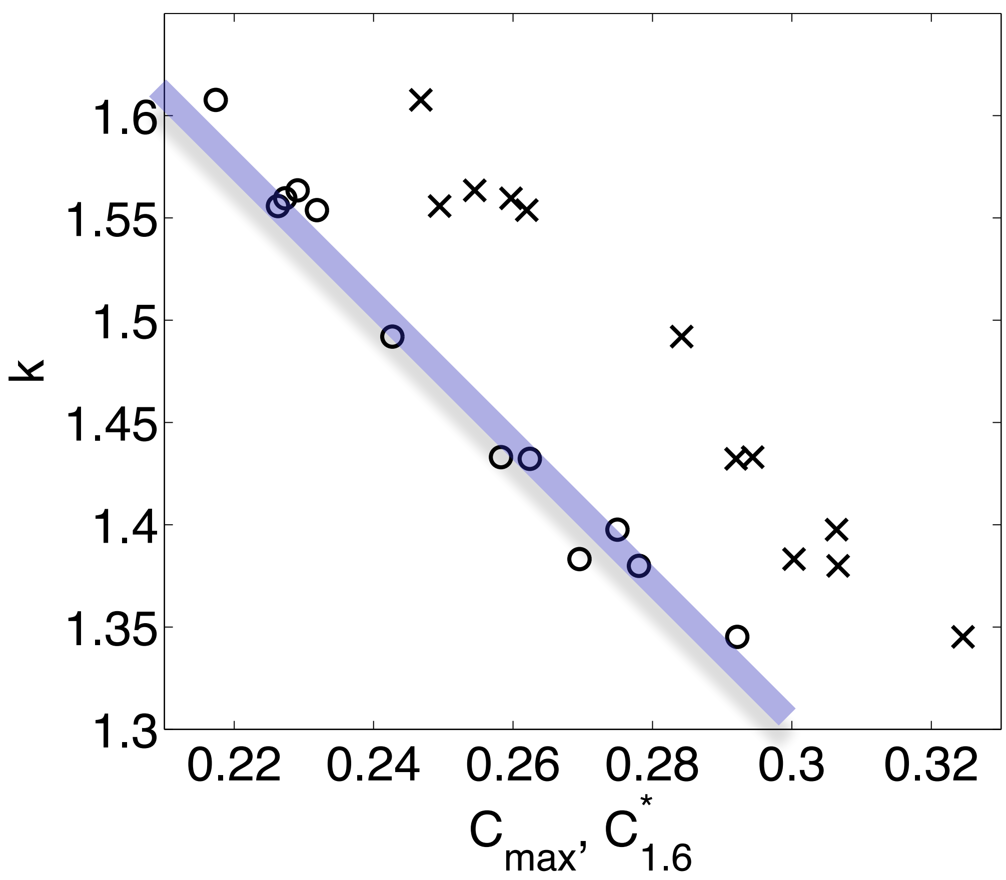

$$C_{\rm max} = (GM_{\rm max})/(c^2 R_{\rm max})$$

Breaking the EOS Degeneracy

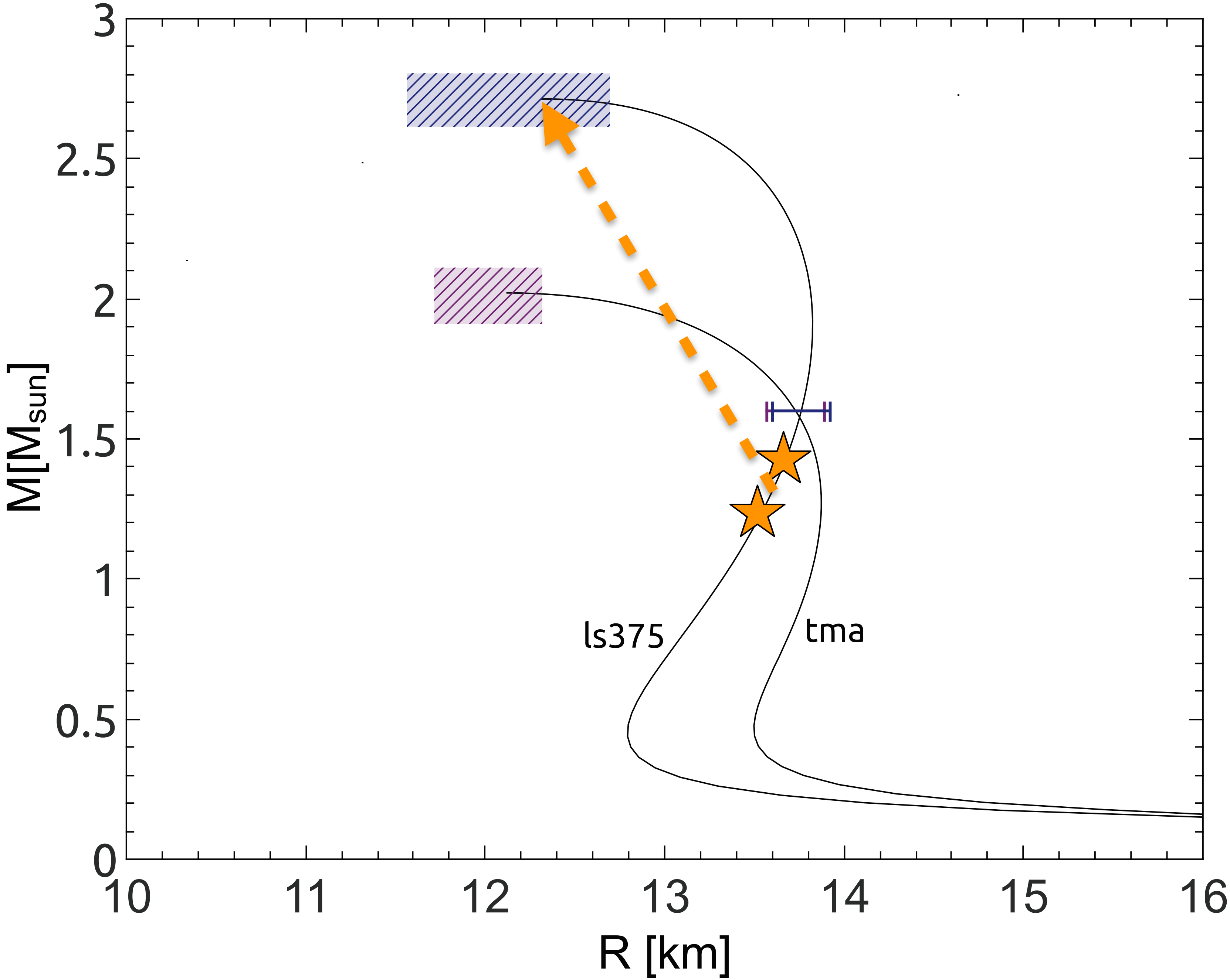

Coherent Wave Burst Analysis

Clark, Bauswein, Cadonati, Janka, Pankow, NS (2014)

Target (noise free)

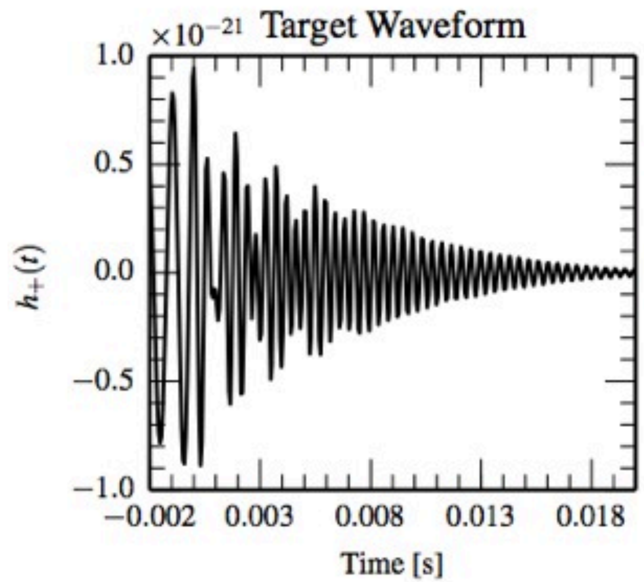

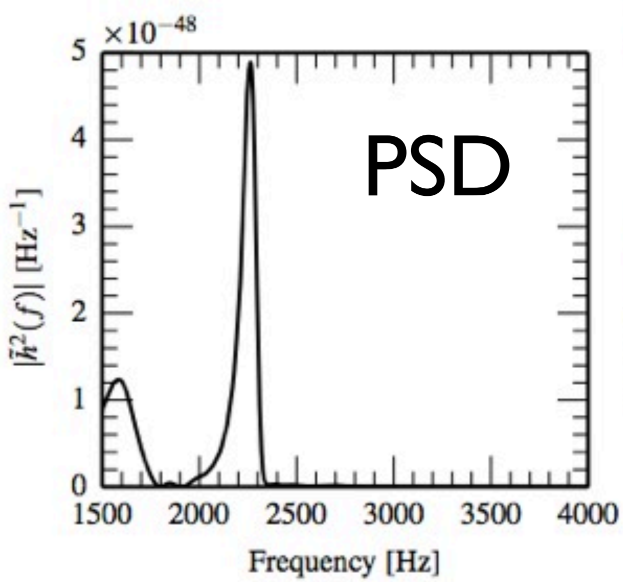

Reconstructions

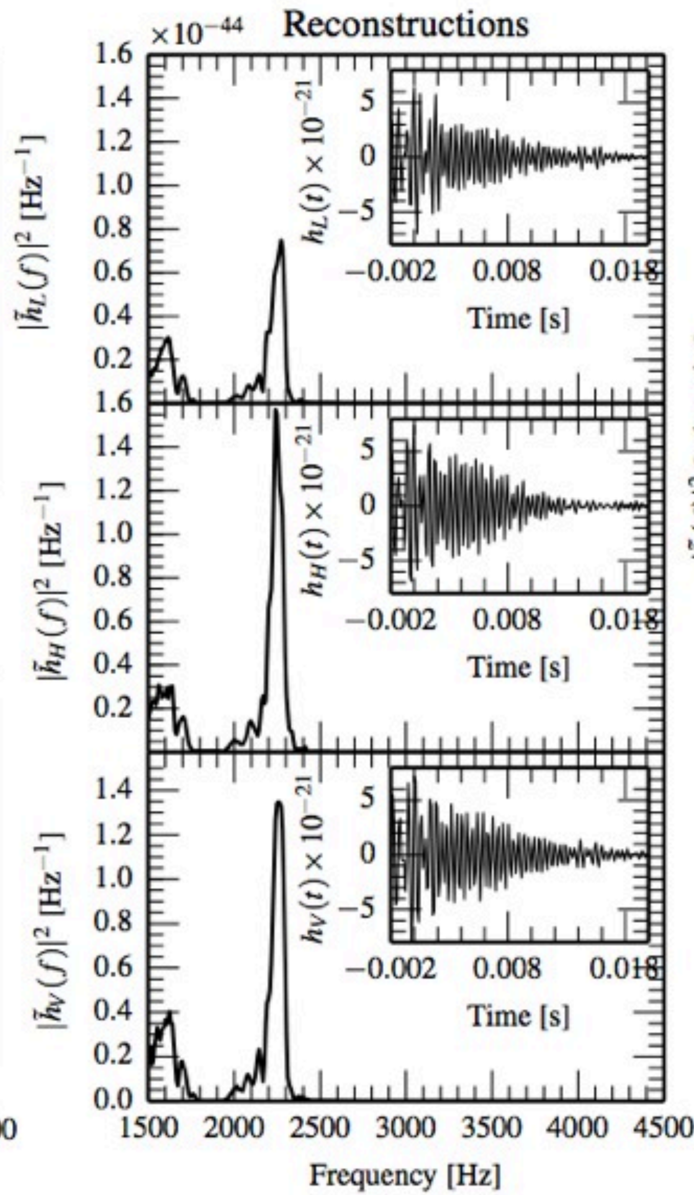

Fit to reconstructed spectrum

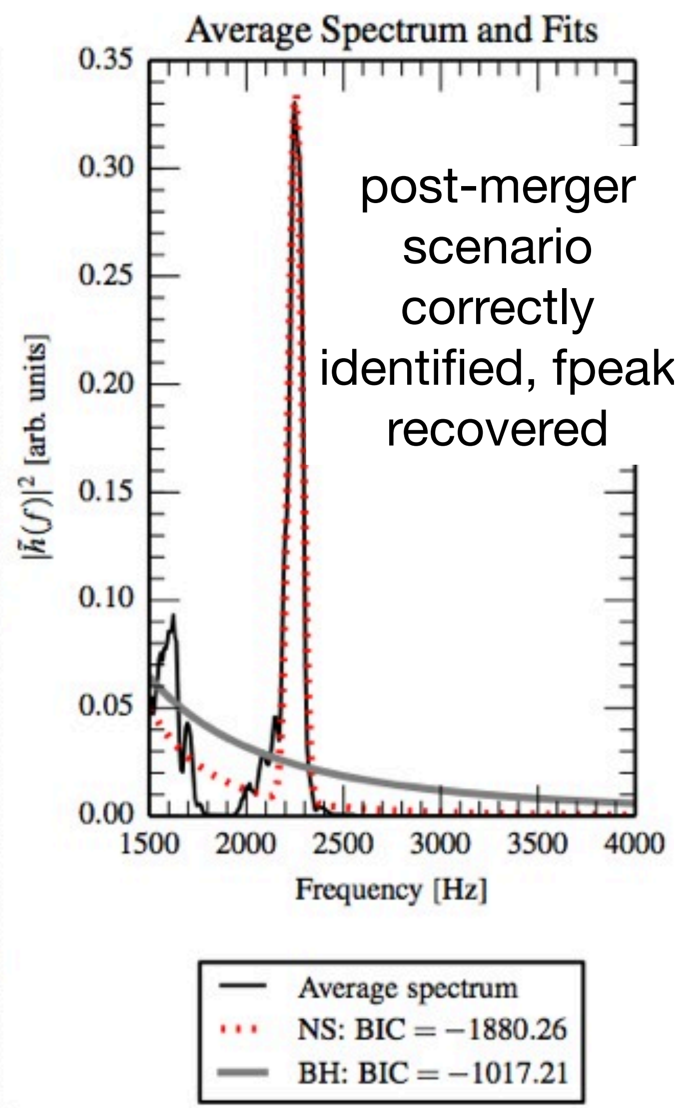

Expected Detection Rate for f_peak

Based on expected *realistic merger rate* per galaxy: 100/Myr

- ***upgraded*** advanced LIGO (assuming 3 times better sensitivity than current advanced LIGO detectors)

  realistic rate for ideal matched filtering:

  ~**1-2**/yr

- Strong motivation for aLIGO and aVIRGO **upgrades**.

Perspectives

Need to construct analytic templates for post-merger emission:

- 3 main **frequencies** + **initial amplitudes** + **damping timescales** + **temporal changes**

- include influence of **unequal masses**

- **alternative theories of gravity**

If radius is first constraint to ~10% by the inspiral GW detections, then the parameter space will be reduced significantly and analytic templates will be easier to obtain within that subspace.

Efficient numerical codes that rely on approximate (but still accurate) solutions, such as SPH + CFC will enable a large parameter study and template construction.

linear + quasi-linear + nonlinear

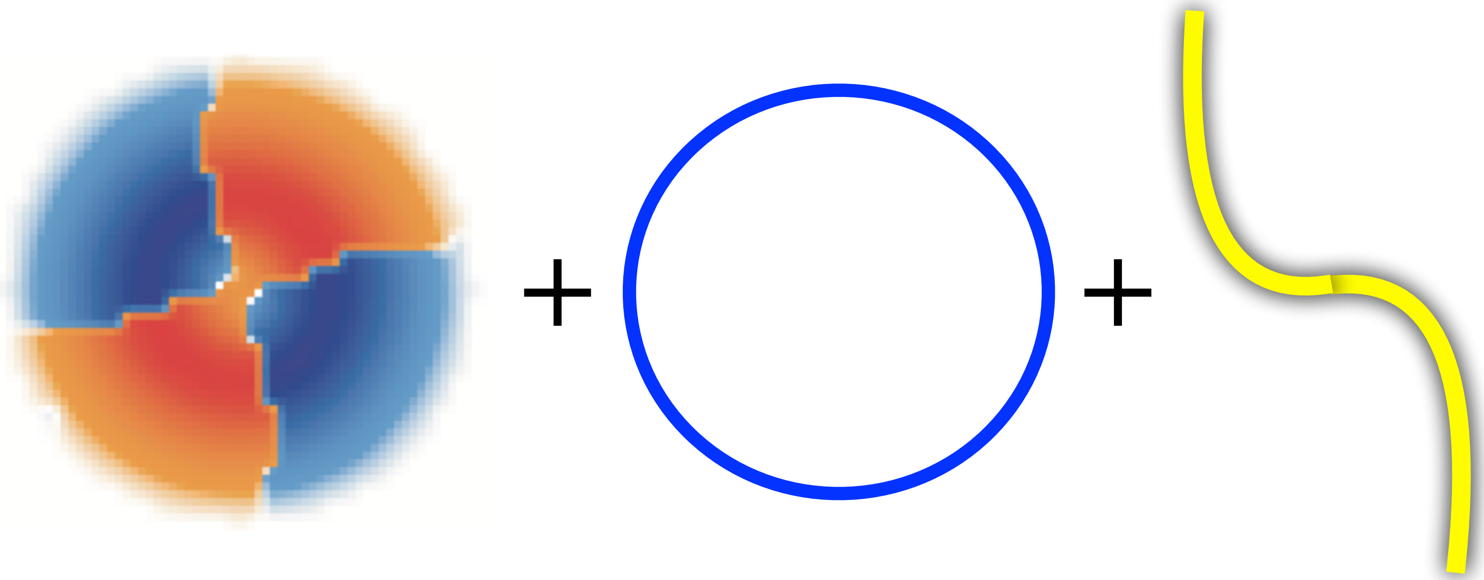

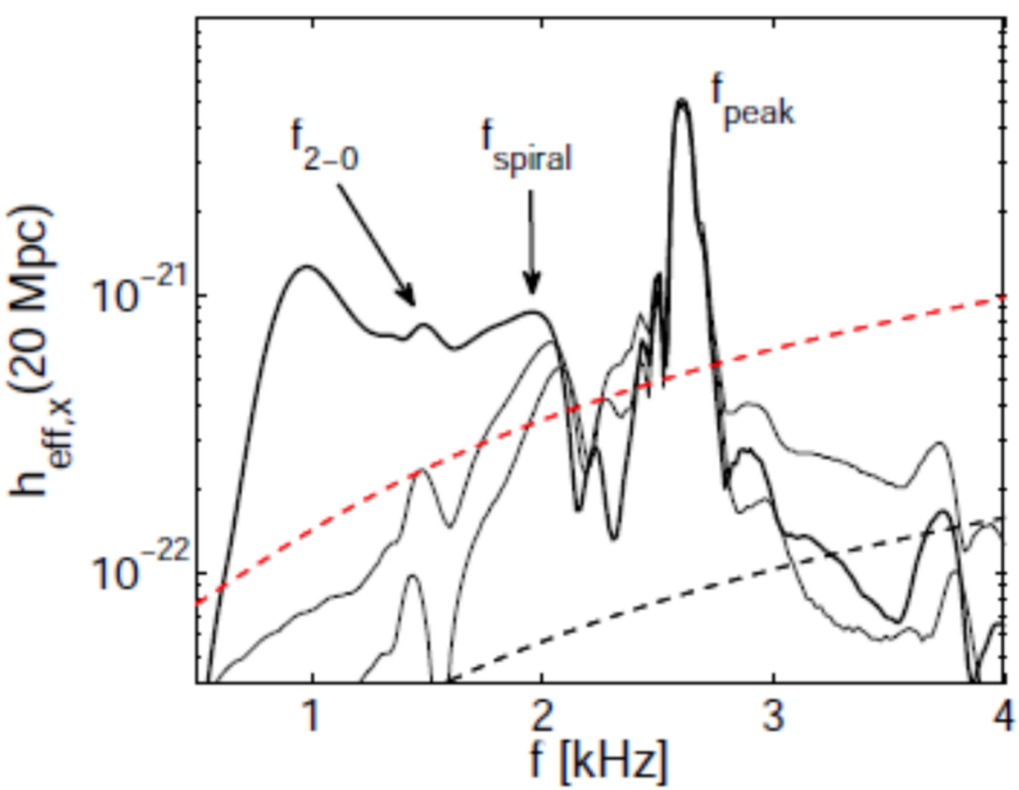

linear + quasi-linear + nonlinear

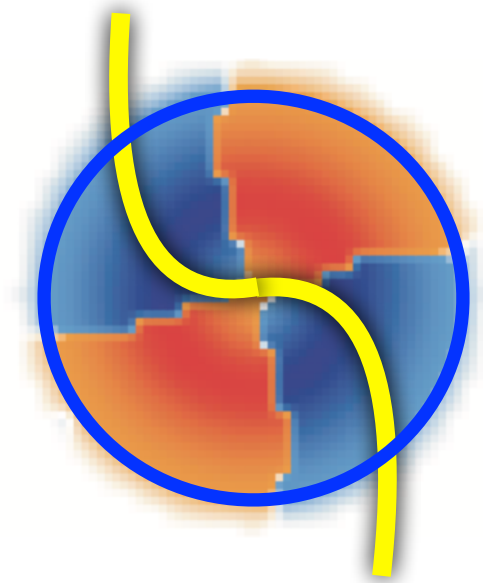

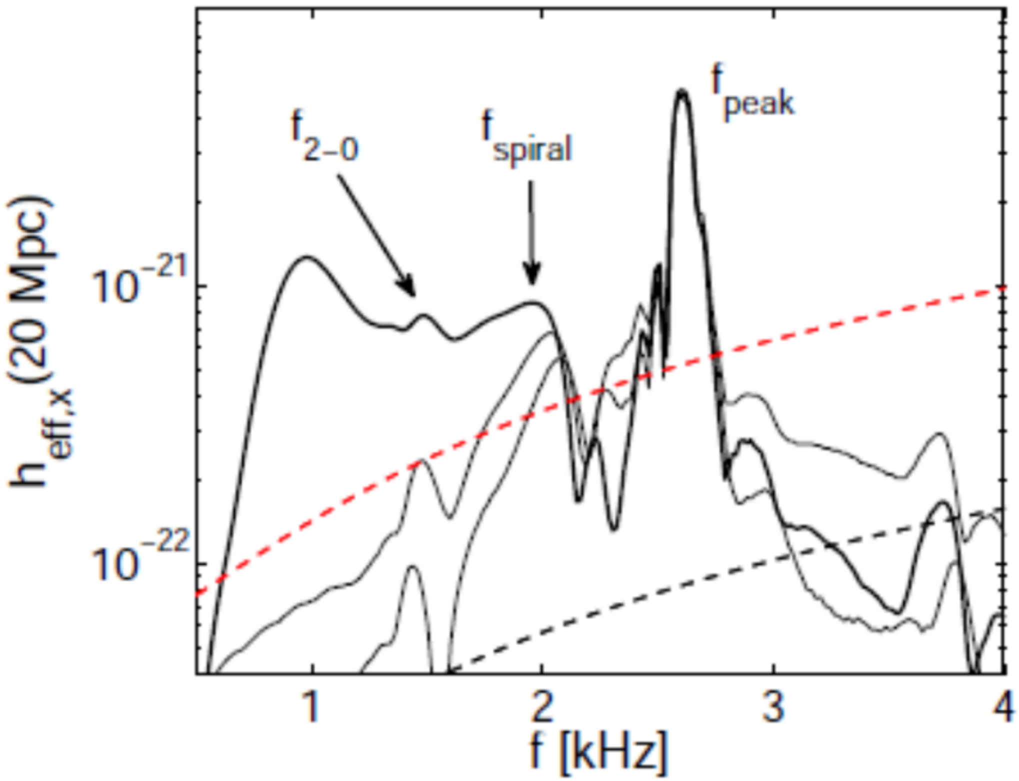

linear + quasi-linear + nonlinear

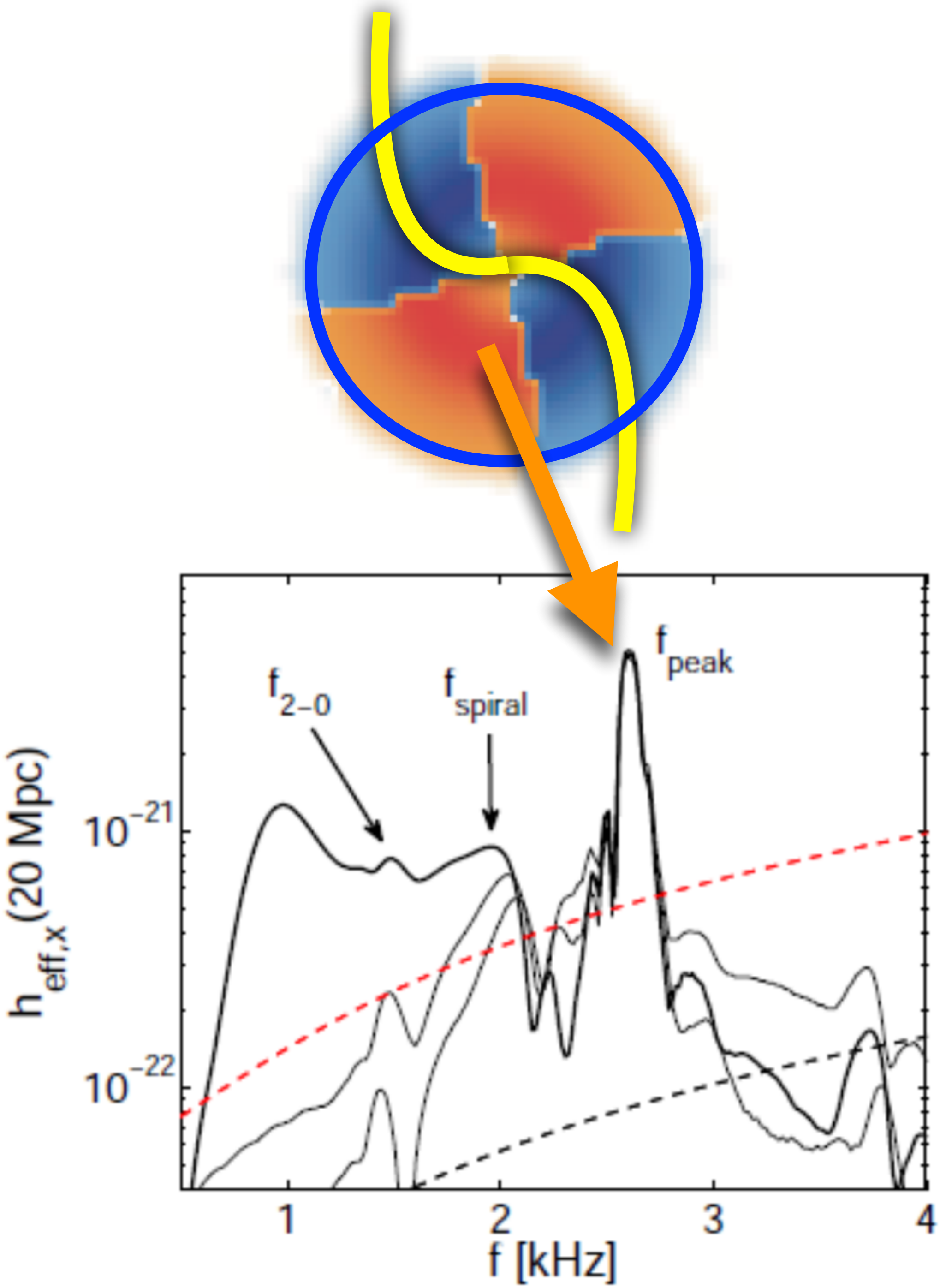

linear + quasi-linear + nonlinear

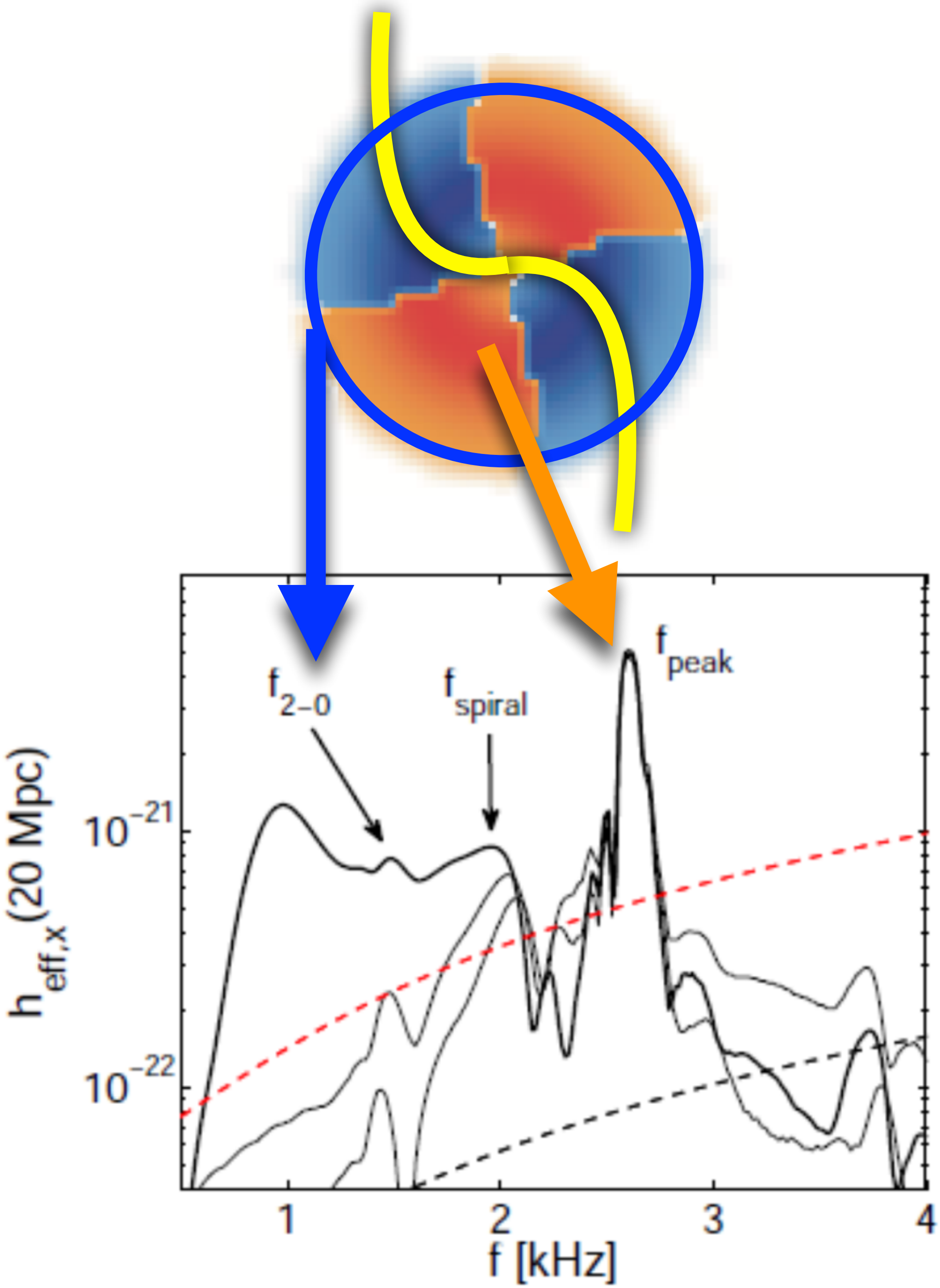

linear + quasi-linear + nonlinear

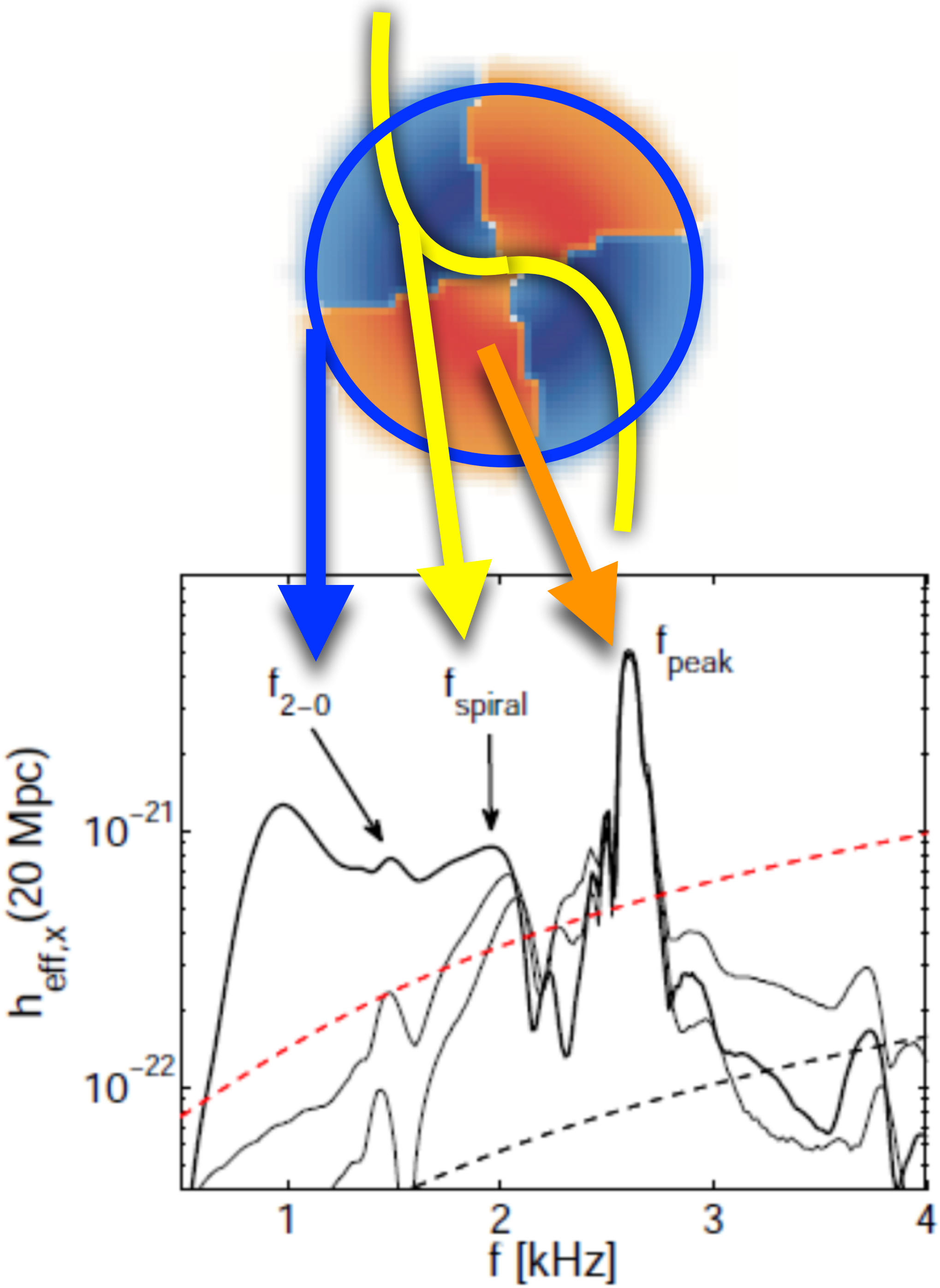

GW Damping Timescale for *f*-Modes

Doneva, Gaertig, Kokkotas, Krueger (2013)

No rotation:

$$\frac{1}{\tau_0[\mathrm{s}]} = \frac{\bar{M}^3}{\bar{R}^4}\left[22.85 - 14.65\frac{\bar{M}}{\bar{R}}\right]$$

When this is applied to the mass and radius of the remnant:

$\tau \sim 200$ ms.

Uniform rotation:

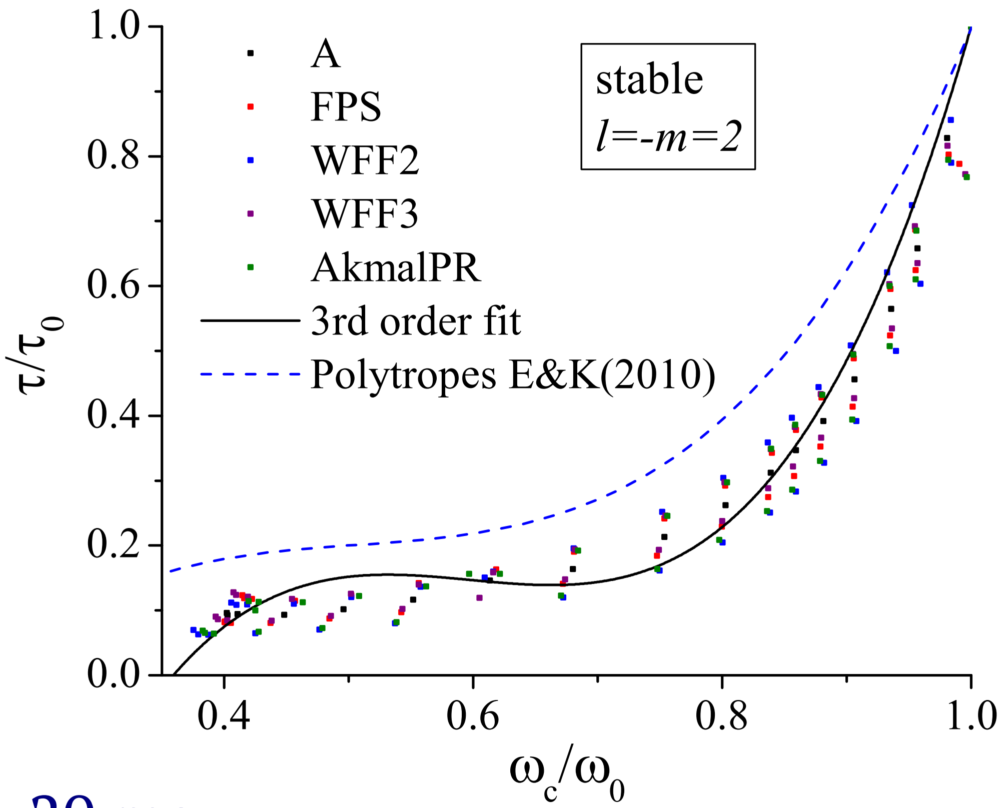

At rapid rotation: we estimate

$\tau \sim \tau_0/10$ i.e. ~ 20 ms.

Real GW timescale is somewhere in between: 20ms < τ <200ms

What is the actual GW damping timescale for f-modes?

Acoustic Damping Timescales for Radial Modes

<u>post-merger:</u>

f_2-0 is damped within
a few ms

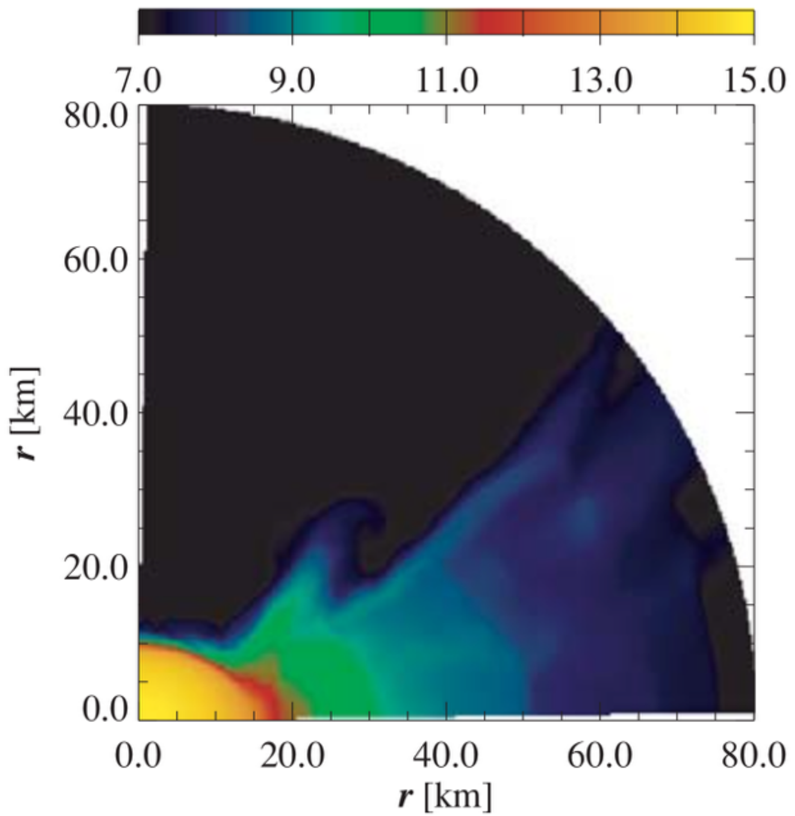

Because the remnant is rapidly rotating, it is **shedding mass** during the radial oscillations.

Sound waves leak into the low-density envelope, which **strongly damps** radial oscillations.

What is the precise timescale? How does it depend on EOS/mass?

Summary

- Post-merger GW asteroseismology is a viable method for constraining the EOS
- Estimated detection rate of a few per year with upgraded aLIGO detectors
- Need to develop templates for complete post-merger evolution, including 3 main frequencies and their damping timescales
- If remnant survives for minutes (magnetar formation?) need to consider gravitational-wave driven (CFS) instabilities

THANK YOU!